

Comparative and functional morphology of wing coupling structures in Trichoptera: Integripalpia

Ian C. Stocks

Department of Entomology, Soils, and Plant Sciences Clemson University, Clemson, South Carolina, 29634, USA; current address: Florida Department of Agriculture and Consumer Services, Department of Plant Industry, 1911 Southwest 34th Street, Gainesville, Florida, 32608, USA (e-mail: stocks@doacs.state.fl.us)

Received 21 Sep. 2009, revised version received 21 Sep. 2010, accepted 28 Sep. 2010

Stocks, I. C. 2010: Comparative and functional morphology of wing coupling structures in Trichoptera: Integripalpia. — *Ann. Zool. Fennici* 47: 351–386.

Trichoptera and several other insect orders have evolved functional diptery while retaining four wings (morphological tetraptery), which results from the interaction of specialized structures that unite the wings. In this contribution, the comparative and functional morphology of the forewing-hindwing coupling apparatuses and related structures in the suborder Integripalpia are presented. The components of the wing coupling apparatuses have varied and complex morphologies and interaction modes, that result in partial to complete wing coupling. Wing coupling has evolved repeatedly within the infraorders Brevitentoria and Plenitentoria, and the morphologies of the wing coupling apparatuses are synapomorphies for several families. Phylogenetic trends are discussed that relate to the evolution of functional diptery, such as the diminution of forewing jugal lobes and hindwing prehumeral setae, reinforcement of wing veins, changes in vein topology and elaboration of wing surface features. A novel at-rest forewing-forewing coupling apparatus that has also evolved repeatedly is described and related to the evolution of wing coupling.

Introduction

This is the second of two contributions that covers the comparative and functional morphology of wing coupling apparatus (WCA) and related structures in the caddisflies (Insecta: Trichoptera). This contribution addresses the suborder Integripalpia, a strongly supported monophylum that is consistently recovered in combined molecular and morphological phylogenetic analyses (Kjer *et al.* 2002, Holzenthal *et al.* 2007a). The reader is referred to the first of the two part series (Stocks 2009) for introductory and back-

ground information on wing coupling in general and a review of Trichoptera phylogeny.

Integripalpia currently comprises 4727 species (Morse 2009), but as with Annulipalpia, the true richness is probably much higher. Phylogenetic analyses recover the two infraorders Brevitentoria and Plenitentoria with high bootstrap values, but further resolution is more problematic. However, current practice, which is adopted here, is to recognize several superfamily-level taxa. Integripalpiian families follow Holzenthal *et al.* (2007a, 2007b) (*see* Fig. 1).

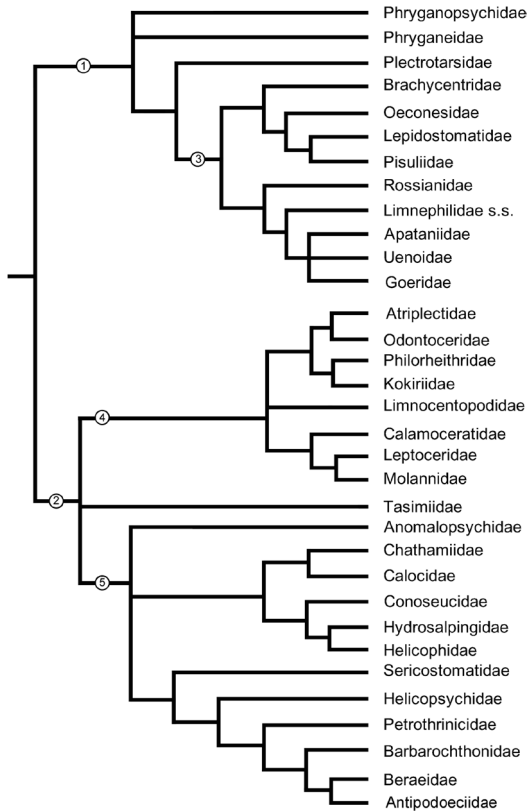


Fig. 1. Phylogeny of Integripalpia. (1) Plenitentoria, (2) Brevitentoria, (3) "Limnephiloidea", (4) "Leptoceroidea", (5) Sericostomatoidea. Modified from Holzenthal *et al.* (2007a, 2007b).

Material and methods

For light microscopy, wings were dissected from the body with the axillary apparatus attached and dehydrated in 100% ethanol. After dehydration, the wings were briefly soaked in clove oil and mounted in Canada balsam. If the wing was to be photographed, the wing vestiture was removed by gently brushing with fine camel hair brushes, taking care not to interfere with putative wing coupling structures. Forewings were typically mounted with the dorsal surface facing ventrally and hindwings with the dorsal surface facing dorsally. Mounting the forewing so that the jugal lobe remained in the extended position (i.e., not reflexed under the wing) required an additional step, adapted from the technique for mounting Thysanoptera. After placing a drop of Canada

balsam on the slide, a cover slip was lowered onto the drop until a thin layer spread onto the cover slip. The cover slip was then removed, inverted, and the forewing placed on the cover slip with the dorsal surface facing dorsally. The wing was manipulated into the correct position with micro pins such that the jugal lobe was extended. With the cover slip in the correct position the slide was gently lowered onto the cover slip. Digital light images were acquired from either a compound or stereo microscope equipped with a ProgRes® C5 digital camera.

For scanning electron microscopy, dissected wings were dehydrated in ethanol, air dried and mounted on stubs with double sided conductive tape. Some wings were degreased in xylene prior to dehydration in ethanol. Specimens were sputter coated with gold in a Denton Vacuum Desk II for 80 seconds, and imaged in a Jeol 5300 ESEM. Screen images were photographed with a digital camera mounted to the SEM camera attachment. Digitally acquired images were manipulated in Adobe Photoshop® for plate assembly. Terminology for wing morphology is based on the works of Schmid (1998), Scheffer (1996), and Huxley and Barnard (1988), except where explained. A list of terms and their abbreviations is given in Table 1. Voucher specimens and slide mounted wings are in the Clemson University Arthropod Collection, Clemson University. The majority of specimens examined were from the Clemson University Arthropod Collection, with additional specimens borrowed from Dr. Oliver Flint (Smithsonian Institution), Dr. Ralph Holzenthal (University of Minnesota) and Dr. Karl Kjer (Rutgers University). When possible, several specimens of each taxon studied were examined to assess for intraspecific variation.

Results

Integripalpia: Brevitentoria

Two superfamily-groups within the infraorder Brevitentoria are conventionally recognized, a monophyletic Sericostomatoidea (twelve families) and a paraphyletic "Leptoceroidea" (eight families; Holzenthal *et al.* 2007a). Structures

either demonstrated or hypothesized to be associated with wing coupling have evolved repeatedly in both “Leptoceroidea” and Sericostomatoidea, and while the wings of taxa in Brevitentoria display a wide variety of morphologies, there is also sufficient morphological consistency to indicate that some characters may prove to be not only taxonomically useful, but phylogenetically informative as synapomorphies.

“Leptoceroidea”

The paraphyletic assemblage “Leptoceroidea” comprises 2215 species in 7 (or 8, pending the position of Tasimiidae) families, but the cosmopolitan family Leptoceridae (1832 species) contains by far the most species (Holzenthall *et al.* 2007b, Morse 2009). The families Calamoceratidae (159 species), Odontoceridae (125 species), and Philorheithridae (29 species) are moderately to strongly-supported monophyla in combined analyses (Kjer *et al.* 2002, Holzenthall *et al.* 2007a, Morse 2009), and a recent analysis recovered Molannidae (37 species) + Calamoceratidae as a monophyletic higher taxon (Holzenthall *et al.* 2007a, Morse 2009).

PHILORHEITHRIDAE

The WCA of this small family is complex and elements of the system fall imperfectly into two functional categories: forewing-hindwing coupling and forewing-forewing coupling. The family is in part diagnosed by “A small, rounded, strongly chitinized extension downwards of the anal margin of the anterior wings near the base” (Mosely 1936). This remarkable structure and its inferred functional role are described in detail below (Fig. 2); Weaver *et al.* (2008) treated this structure as a family level synapomorphy.

The forewing coupling component is essentially similar to that of Odontoceridae (e.g., *Marilia* spp., *Psilotreta* spp.) in that the forewing coupling setae arise as a linear series of curved setae that are in the same plane as the wing membrane. They arise from what is probably a vein, but since the nerve that typically occurs within the interior of the vein could not

be discerned (author’s unpubl. observations), it remains unclear whether the structure is one of the anal group veins; I provisionally name it A3. The forewing coupling setae basally are in a multiserial row but distally become restricted to an evenly spaced and overlapping single row that is approximate to ambient costa; a narrow space without setae is discernable between A3 and ambient costa (Figs. 3 and 4).

The hindwing coupling setae arise from costa and project approximately at right angles to the plane of the wing; the setae are evenly curved, adorned with serrated longitudinal flutes, and gradually decrease in length basally to distally (Figs. 5–8). Presumably the coupling mechanism relies on the hindwing coupling setae curving over and behind the forewing coupling setae.

The forewing lobe adjacent to the costal angle is presumed to be a homologue, albeit greatly enlarged, of a structure found in a similar position in other leptoceroid taxa, such as Leptoceridae, Calamoceratidae and Odontoceridae. The lobe in *Kosrheithrus tillyardi* Mosely is

Table 1. Wing morphology abbreviations.

Abbreviation	Term
A1, A2, A3	anal 1, 2, 3 (vein)
A1+2+3	anal veins 1+2+3
ac	ambient costa (vein)
axc	axillary cord
ba	basal apophysis
C	costa (vein)
Cu1, Cu2	cubitus 1, 2 (vein)
ds	denticulate setae
fwcs	forewing coupling setae
fwA	forewing Anal (vein)
fwm	forewing microtrichia
hv	humeral vein
hwC	hindwing costa (vein)
hwcs	hindwing coupling setae
hwSc	hindwing subcosta (vein)
jl	jugal lobe
jlF	jugal lobe furrow
M	media (vein)
mm	major microtrichia
phs	prehumeral setae
pv	pseudovein
vm	ventral microtrichia
R	radius (vein)
Rs	radius sector
Sc	subcosta (vein)
WCA	wing coupling apparatus

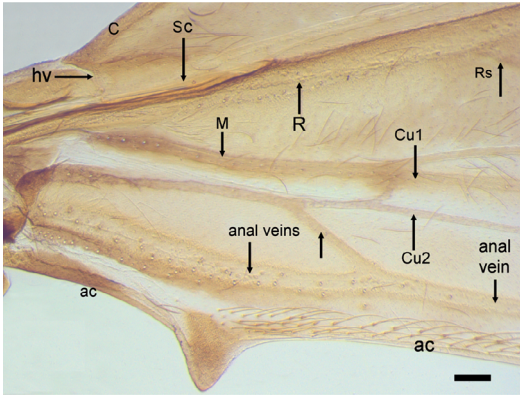


Fig. 2. LM of the left forewing of *Austrheithrus dubitans* Mosely (Philorheithridae), ventral view. Scale bar = 1 mm.

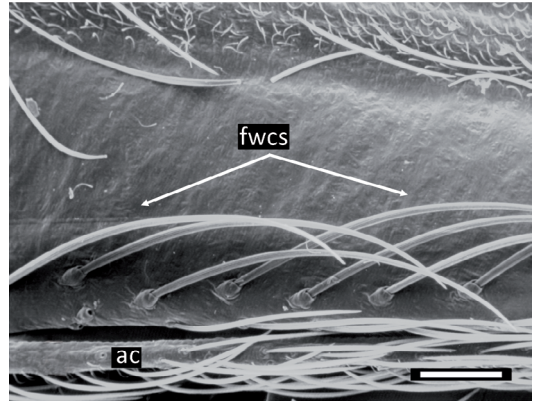


Fig. 3. SEM of the left forewing of *Austrheithrus dubitans* Mosely (Philorheithridae), showing coupling setae, ventral view. Scale bar = 100 μ m.

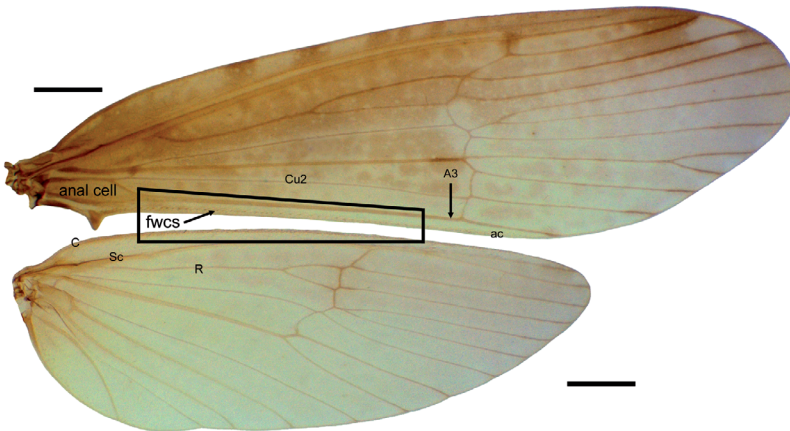


Fig. 4. LM of the left fore- and hindwings of *Austrheithrus dubitans* Mosely (Philorheithridae), ventral view. Boxed area indicates region where the fore- and hindwing coupling seta come into contact. Scale bar = 1 mm.

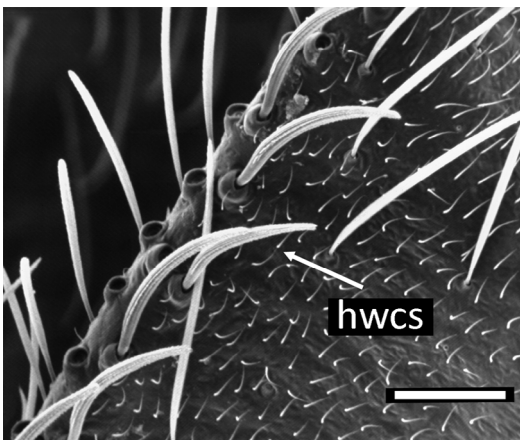


Fig. 5. SEM of the right hindwing coupling setae of *Kosrheithrus tillyardi* Mosely (Philorheithridae), dorsal view. Scale bar = 50 μ m.

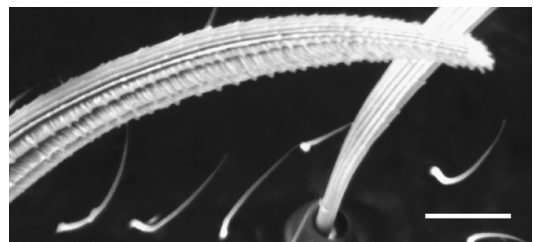


Fig. 6. SEM of the right hindwing coupling setae of *Kosrheithrus tillyardi* Mosely (Philorheithridae), dorsal view. Scale bar = 10 μ m.

roughly circular in outline (Figs. 9–11) and in *Austrheithrus dubitans* Mosely is more triangular (Figs. 2 and 4). The margin is continuous with ambient costa but an additional structure of unknown affinity also attaches to the lobe

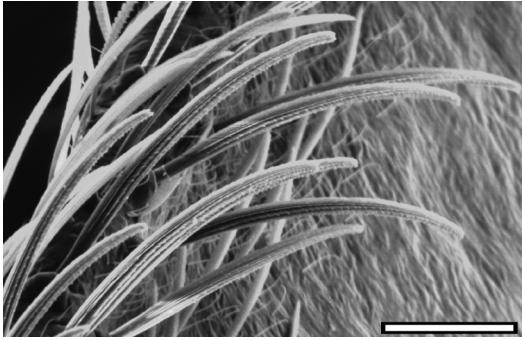


Fig. 7. SEM of the right hindwing coupling setae of *Kosrheithrus tillyardi* Mosely (Philorheithridae), dorsal view. Scale bar = 50 μm .

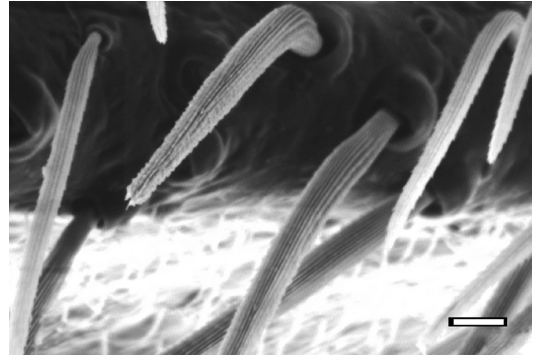


Fig. 8. SEM of the right hindwing coupling setae of *Kosrheithrus tillyardi* Mosely (Philorheithridae), dorsal view. Scale bar = 10 μm .

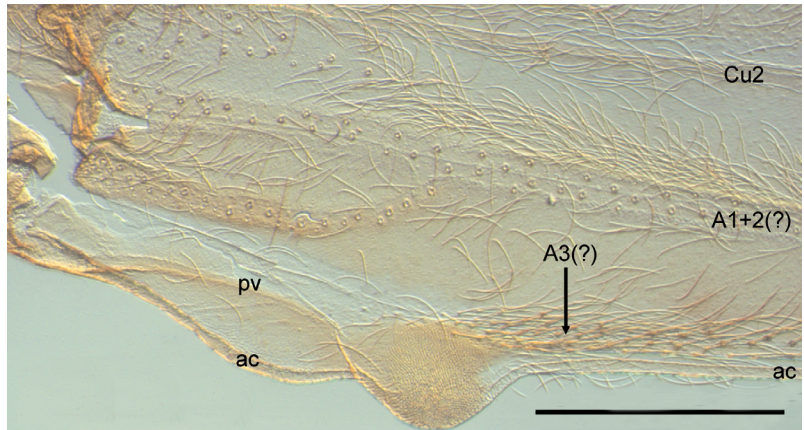


Fig. 9. LM of the left forewing anal angle region of *Kosrheithrus tillyardi* Mosely (Philorheithridae), ventral view. Scale bar = 1 mm.

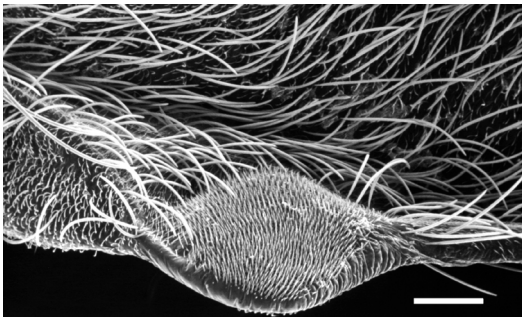


Fig. 10. SEM of the left forewing anal angle lobe of *Kosrheithrus tillyardi* Mosely (Philorheithridae), ventral view. Scale bar = 100 μm .

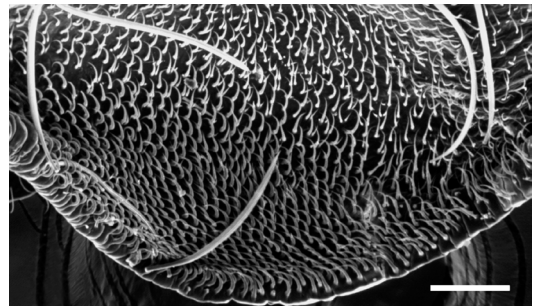


Fig. 11. SEM of the left forewing anal angle lobe of *Kosrheithrus tillyardi* Mosely (Philorheithridae), ventral view. Scale bar = 50 μm .

basally (pseudovein (pv) Fig. 9). The lobe is meniscus-shaped (ventrally concave, dorsally convex) with each face presenting a field of microtrichia (Figs. 10 and 11). The ventral face is adorned with microtrichia that are distinctly curved and oriented locally in a uniform manner,

but globally over the ventral surface they gradually change their orientation; dorsally the microtrichia are simply acuminate (Fig. 12).

There may be some role for this structure in forewing-hindwing coupling, but probably the primary role is forewing-forewing coupling while

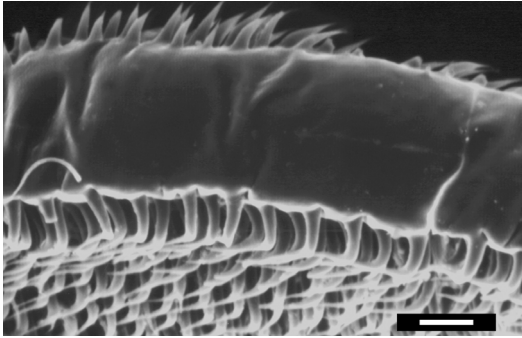


Fig. 12. SEM of the left forewing anal angle lobe of *Kosrheithrus tillyardi* Mosely (Philorheithridae), ventral view. Scale bar = 10 μ m.

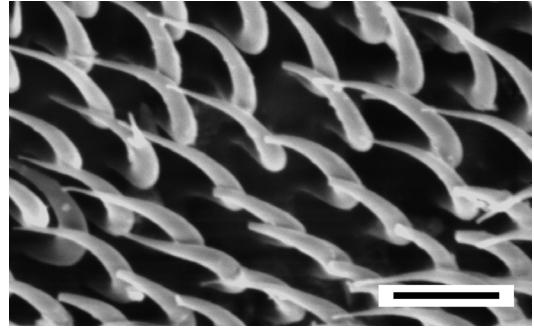


Fig. 13. SEM of the left forewing anal angle lobe of *Kosrheithrus tillyardi* Mosely (Philorheithridae), ventral view. Scale bar = 10 μ m.

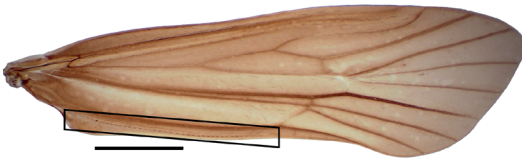


Fig. 14. LM of the left forewing of *Marilia* sp. (Odontoceridae), ventral view. Boxed region emphasizes area with coupling setae. Scale bar = 1 mm.

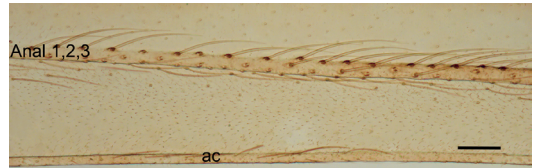


Fig. 15. LM of the left forewing coupling setae of *Psilotreta* sp. (Odontoceridae), ventral view. Scale bar = 100 μ m.

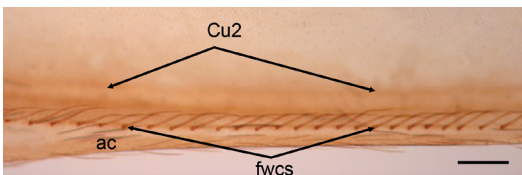


Fig. 16. LM of the left forewing coupling setae of *Marilia flexuosa* Ulmer (Odontoceridae), ventral view. Scale bar = 100 μ m.

the wings are at rest, similar to that of the microtrichia fields described for *Smicridea* sp. (Stocks 2009). The biomechanical principle appears to rely on the fact that the lobes are dorso-ventrally menisciform in shape, which allows the dorsal surface of one lobe to rest on the ventral surface of the opposite lobe. The two opposing fields of microtrichia are then approximate and become entangled. Entanglement, and therefore stability, is probably enhanced by the fact that the microtrichia are strongly curved and pointed (Figs. 12 and 13). There are few ecological or behavior observations on adults that could shed light on the role of coupled forewings, but philorheithrids are known to rest on twigs with their wings held tightly to the body, similar to that attained by

Molannidae when at rest. Alternatively, or additionally, wings closely attached to the body might enable the animals to move through tight underbrush more efficiently or with decreased risk of damage to the wings, an ecological role similar to that in *Merope tuber* Newman (Mecoptera: Meropeidae; Hlavac 1974).

ODONTOCERIDAE

The WCA of Odontoceridae is biomechanically similar to that of Philorheithridae, but *in vitro* manipulations suggest that it is substantially more efficient at influencing the coupling. The position of the anal vein relative to ambient costa varies among taxa, being very close to the latter in *Marilia* spp. (Fig. 14) and positioned more anteriorly in *Psilotreta* spp. (Fig. 15). The forewing coupling setae in *Marilia* spp. originate near the anal angle and progress distally into a single row of setae that are evenly spaced, and with each successive seta acquiring a sinusoidal shape; the emergent shape defines a ledge that engages the hindwing costal setae (Figs. 16 and 17). The row in *Psilotreta* spp. is less even

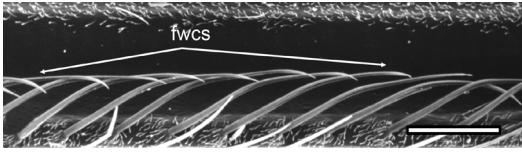


Fig. 17. SEM of the left forewing coupling setae of *Marilia flexuosa* Ulmer (Odontoceridae), ventral view. Scale bar = 100 μm .

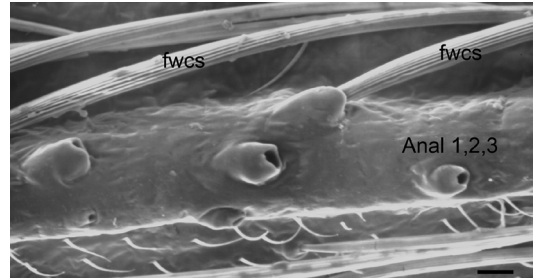


Fig. 18. SEM of the left forewing coupling setae of *Psilotreta* sp. (Odontoceridae), ventral view. Scale bar = 10 μm .

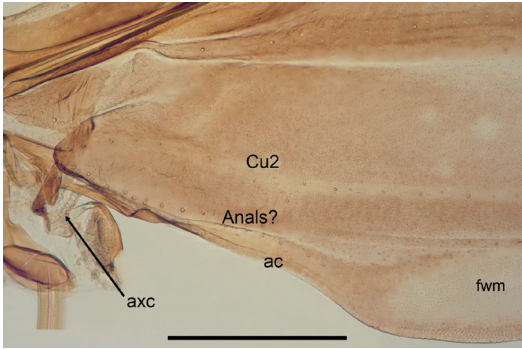


Fig. 19. LM of the left forewing anal angle of *Marilia* sp. (Odontoceridae), ventral view. Scale bar = 0.5 mm.

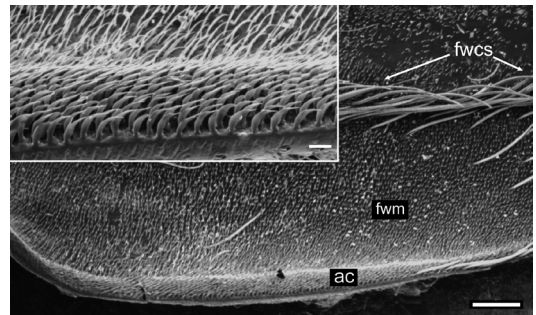


Fig. 20. SEM of the left forewing anal angle of *Marilia flexuosa* Ulmer (Odontoceridae), ventral view. Scale bar = 100 μm . Inset of microtrichia. Scale bar = 10 μm .

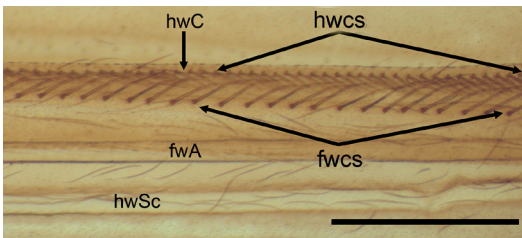


Fig. 21. LM of left coupled wings of *Marilia flexuosa* Ulmer (Odontoceridae) *in vitro*, ventral view. Scale bar = 0.5 mm.

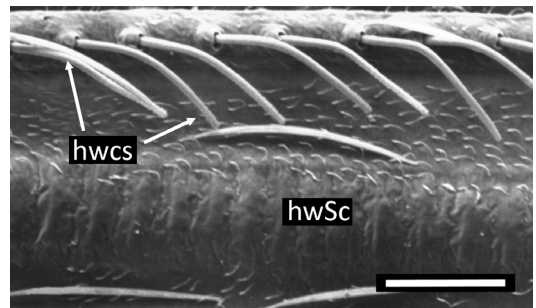


Fig. 22. SEM of the right hindwing coupling setae of *Marilia flexuosa* Ulmer (Odontoceridae), dorsal view. Scale bar = 50 μm .

and apparently borne on the anal vein (Fig. 18); although one row is structurally dominant, other setae are distributed on the vein. The forewing ventral anal angle is less developed in *Marilia* sp. than that of Philorheithridae but has the same basic structure and is adorned, at least ventrally, with microtrichia that are similar in shape to those of *Kosrheithrus tillyardi* Mosely (Figs. 19 and 20). The hindwing coupling setae of *Marilia* sp. are considerably more robust than those of *K. tillyardi* and are more regularly shaped and spaced. As with the forewing coupling setae, the hindwing coupling setae arise from a ledge-like

structure that projects slightly from the plane of the wing membrane (Figs. 21–25). A second row of apically oriented and evenly distributed setae arise from the hindwing subcosta in the region opposite the costal row, and may also be involved in coupling (Figs. 24 and 26). The biomechanical basis appears to be that of two interlocking “J-grooves,” one on the forewing and the other on the hindwing.

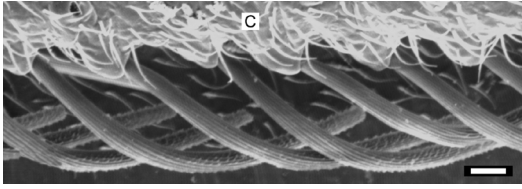


Fig. 23. SEM of the right hindwing coupling setae of *Marilia flexuosa* Ulmer (Odontoceridae), dorsal view. Scale bar = 10 μ m.

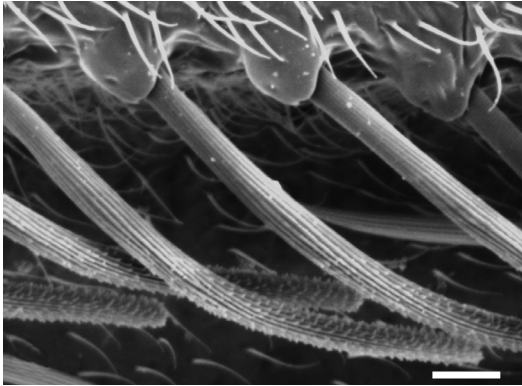


Fig. 25. SEM of the right hindwing coupling setae of *Marilia flexuosa* Ulmer (Odontoceridae), dorsal view. Scale bar = 10 μ m.

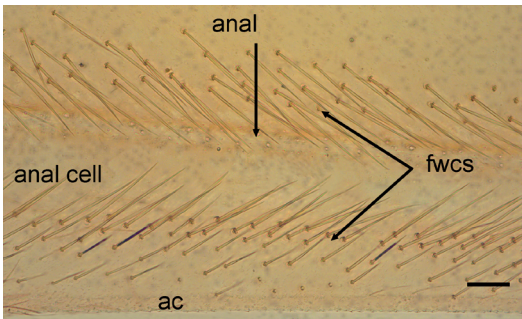


Fig. 27. LM of the left forewing coupling setae of *Heteroplectron americanum* (Walker) (Calamoceratidae), ventral view. Scale bar = 100 μ m.

CALAMOCERATIDAE

The WCA of Calamoceratidae is biomechanically unique in Trichoptera and appears to be a synapomorphy for the family. The forewing coupling setae occur in two patches, one arising from or near ambient costa, and a partner patch arising from or posterior to Cu2 (Figs. 27–30). The anal angle is adorned with modi-

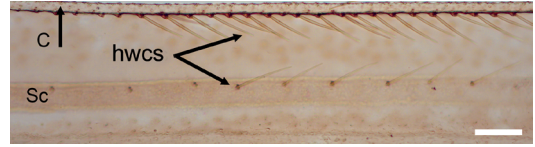


Fig. 24. LM of the right hindwing coupling setae of *Marilia flexuosa* Ulmer (Odontoceridae), dorsal view. Scale bar = 100 μ m.

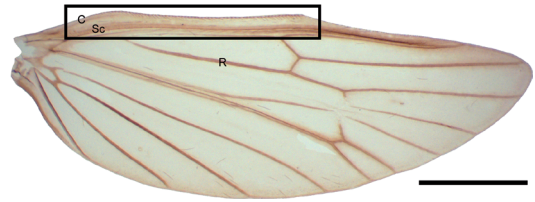


Fig. 26. LM of the left hindwing of *Marilia flexuosa* Ulmer (Odontoceridae), ventral view. Boxed area is the region on costa containing the forewing coupling setae. Scale bar = 1 mm.

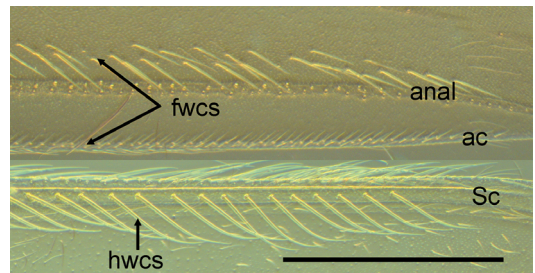


Fig. 28. LM of the left forewing coupling setae and hindwing coupling setae of *Phylloicus* sp., ventral view. Scale bar = 1 mm.

fied microtrichia that are elongate-acuminate in shape and that project obliquely toward the anterodistal margin of the wing (Figs. 31 and 32). The morphology of the socketed setae that populate the two opposing forewing patches is variable among taxa. In the forewing of both *A. pyraloides* and *H. americanum*, the anterior patch arises immediately anterior to the A1+2+3 vein, but in both taxa they are elongate-acuminate and project obliquely in a posterodistal direction (Fig. 33). In *Anisocentropus pyraloides* (Walker) the setae in the opposing patch arise from ambient costa and are relatively short and stout with the distal third markedly serrate-acuminate (Fig. 34), while in *Heteroplectron americanum* (Walker) the setae emerge from within

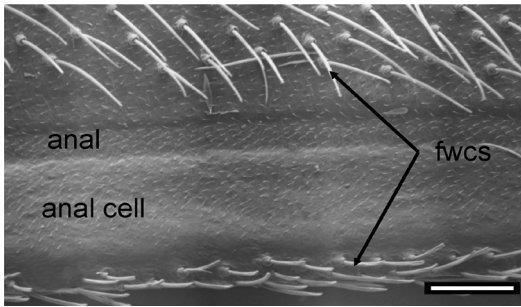


Fig. 29. SEM of the left forewing coupling setae of *Anisocentropus pyraloides* (Walker) (Calamoceratidae), ventral view. Scale bar = 100 μ m.

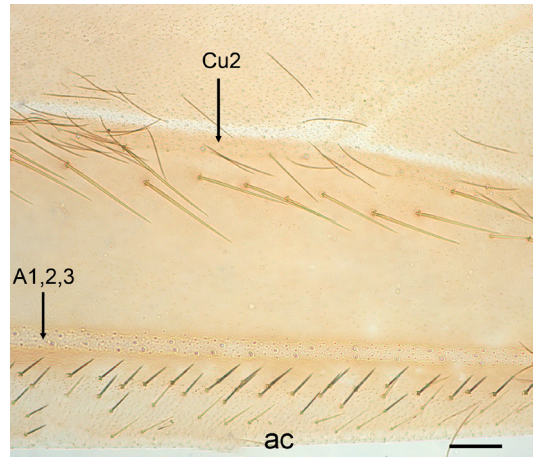


Fig. 30. LM of the left forewing anal cell region of *Georigium japonicum* (Ulmer) (Calamoceratidae), ventral view. Scale bar = 100 μ m.

Fig. 31. LM of the left forewing of *Phylloicus* sp., ventral view. A = region of acanthae on the anal angle, B = region of forewing coupling setae. Scale bar = 1 mm.

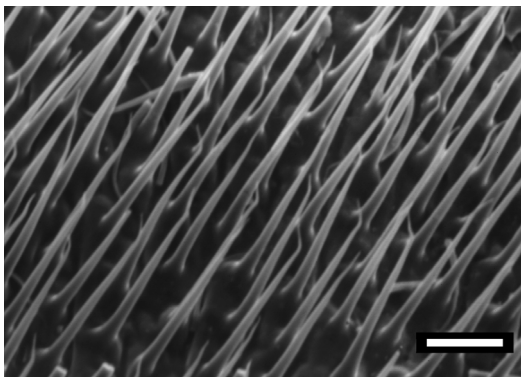
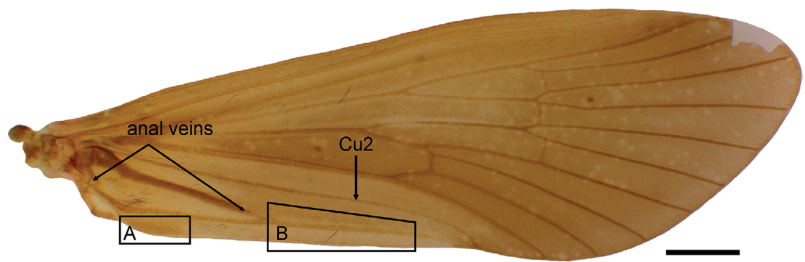


Fig. 32. SEM of the left forewing anal angle region of *Anisocentropus pyraloides* (Walker) (Calamoceratidae), ventral view. Scale bar = 10 μ m.

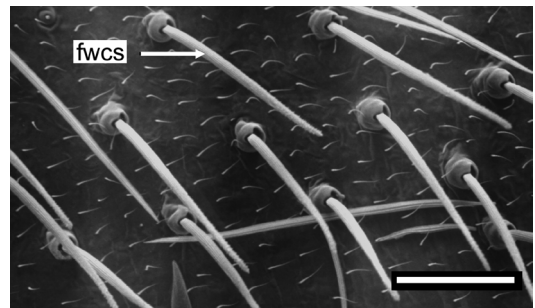


Fig. 33. SEM of the left forewing coupling setae of *Anisocentropus pyraloides* (Walker) (Calamoceratidae), ventral view. Scale bar = 50 μ m.

the anal cell and are elongate-acuminate (Fig. 27); in both taxa, they project in a predominantly distal direction.

The hindwing partner component is comprised of two morphologically distinct types of setae, one of which arises basally on and near

the humeral angle (Figs. 35 and 36), and one of which arises from subcosta in the region anatomically opposite the distal forewing component (Figs. 37 and 38). The setae located near the humeral area are elongate tapering structures that are distinctively adorned with triangular denticles and bear an overall resemblance to those found in Hydropsychidae: Macronemati-

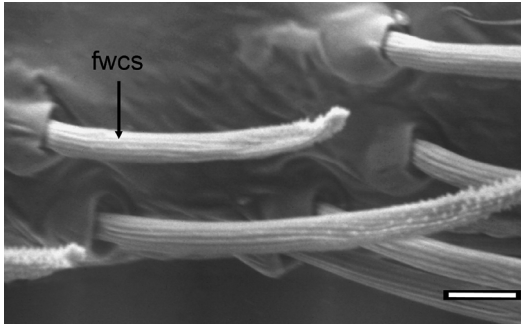


Fig. 34. SEM of the left forewing coupling setae of *Anisocentropus pyraloides* (Walker) (Calamoceratidae), ventral view. Scale bar = 10 μ m.

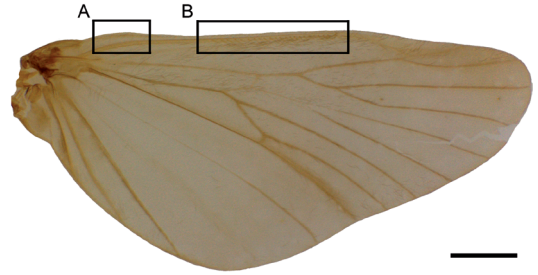


Fig. 35. LM of the right hindwing of *Phylloicus* sp., dorsal view. A = region of denticulate setae shown in Fig. 36, B = region of hindwing coupling setae in Figs. 37 and 38. Scale bar = 1 mm.

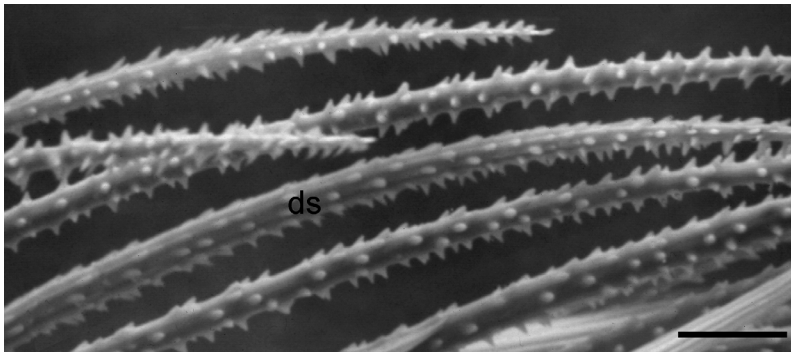


Fig. 36. SEM of the basal setae on the right hindwing of *Anisocentropus pyraloides* (Walker) (Calamoceratidae), dorsal view. Scale bar = 10 μ m.

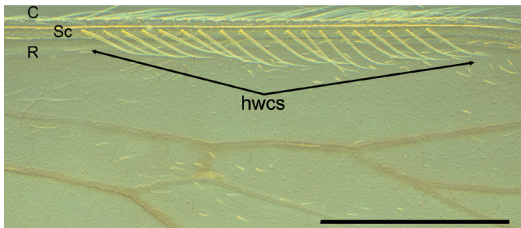


Fig. 37. LM of the right hindwing coupling setae of *Phylloicus* sp., dorsal view. Scale bar = 1 mm.

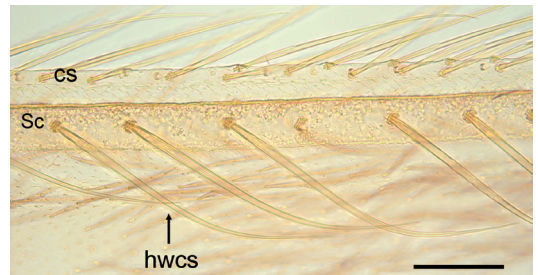


Fig. 38. LM of the right hindwing coupling setae of *Phylloicus* sp., dorsal view. Scale bar = 1 mm.

nae (Stocks 2009). No functional role was suggested by *in vitro* manipulation, but their position and sculpture suggest that they may have a role in meshing with the bed of microtrichia on the anal angle of the forewing. The setae on subcosta appear to be the primary structures that ensure wing coupling. A biomechanical model of this system is not obvious, but the interaction may rely on the hindwing coupling setae either gliding above, or becoming entangled within, the forewing ambient costal setae. The motion of the wings during the upward and anterior

trajectory would suggest that the forewing setae “drag” the hindwing coupling setae along when they come into contact; similarly, the forewing setae between Cu2 and A1+2+3 may “push” against the hindwing costal margin during the down stroke. Alternatively, the two patches of forewing setae “trap” the hindwing costal and subcostal coupling setae during the wing stroke such that the coupling setae become more or less randomly entangled between the two patches.

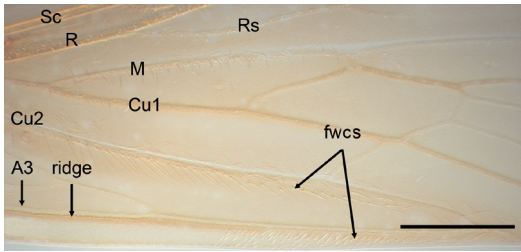


Fig. 39. Light micrograph of the left forewing of *Georgium japonicum* (Ulmer) (Calamoceratidae), ventral view. Scale bar = 1 mm.

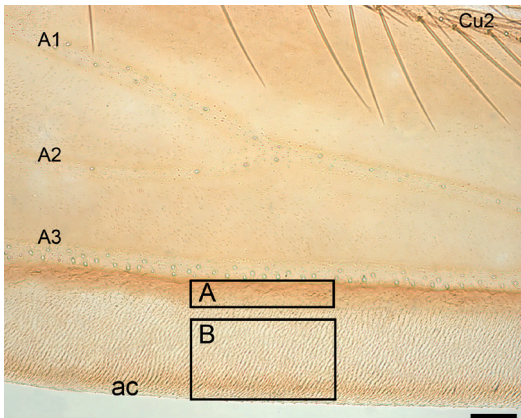


Fig. 41. LM of the left forewing anal angle and anal cell region of *Georgium japonicum* (Ulmer) (Calamoceratidae), ventral view. A = region of microtrichia, B = region of sclerotized cuticle posterior to A1+2+3. Scale bar = 100 μ m.

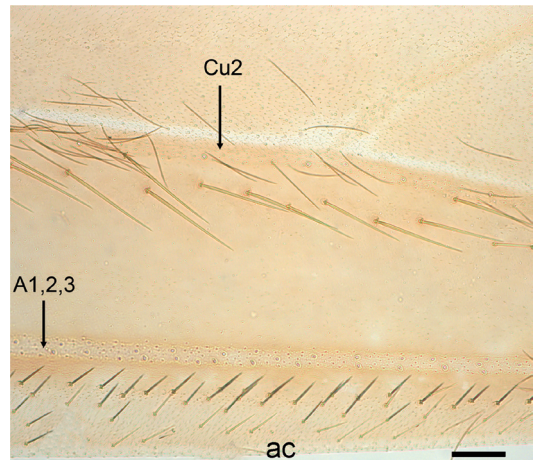
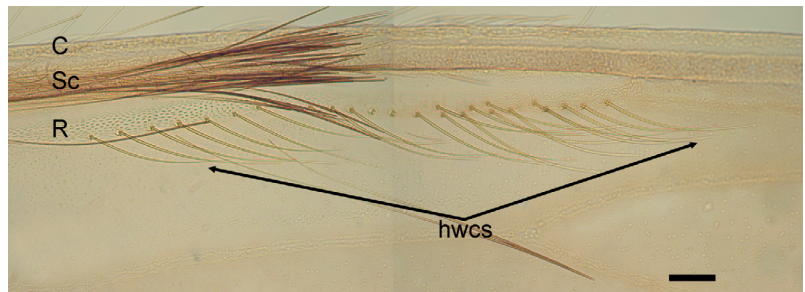


Fig. 40. LM of the left forewing of *Georgium japonicum* (Ulmer) (Calamoceratidae), ventral view. Scale bar = 1 mm.



Fig. 42. LM of the right hindwing coupling setae on subcosta of *Georgium japonicum* (Ulmer) (Calamoceratidae), dorsal view. Scale bar = 100 μ m.

Fig. 43. LM of the right hindwing coupling setae on Radius of *Georgium japonicum* (Ulmer) (Calamoceratidae), dorsal view. Scale bar = 100 μ m.



A somewhat modified system occurs in *Georgium japonicum* (Ulmer). The forewing anal patch of coupling setae is restricted to the apical half of the anal cell (Fig. 39); the setae arise entirely in the anal cell membrane, and are comparatively shorter than those of *H. americanum* (Fig. 40). The basal region of the anal cell contains an enlarged patch of microtrichia (Fig. 41), which is limited anteriorly by

a longitudinal sclerotized region immediately posterior to A1+2+3, and ends abruptly where the patch of microtrichia begins. The hindwing possesses several types of setae and inferring a biomechanical model is more complicated (Figs. 42 and 43). The setae morphologically most similar (homologous?) to those of *A. pyraloides* and *H. americanum* arise not from subcosta but from Radius, again in a position anatomically

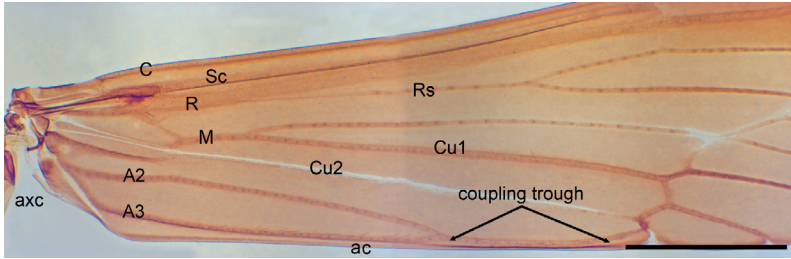


Fig. 44. LM of the left forewing of *Mystacides pacifica* Mey (Leptoceridae), showing coupling trough, ventral view. Scale bar = 1 mm.

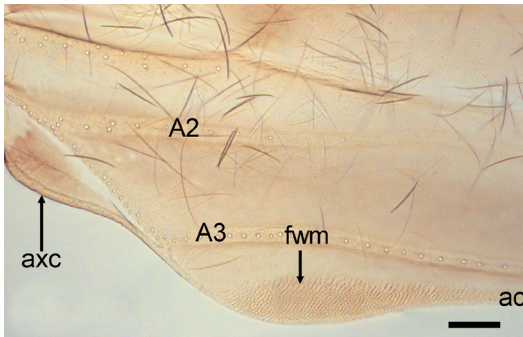


Fig. 45. LM of the left forewing ventral anal angle of *Triaenodes* sp. (Leptoceridae), ventral view. Scale bar = 100 μ m.

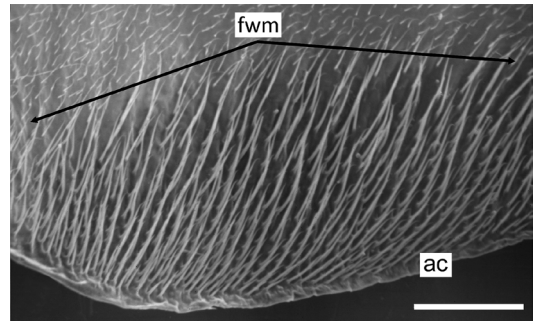


Fig. 46. SEM of the left forewing anal angle of *Oecetis avara* (Banks) (Leptoceridae), ventral view. Scale bar = 50 μ m.

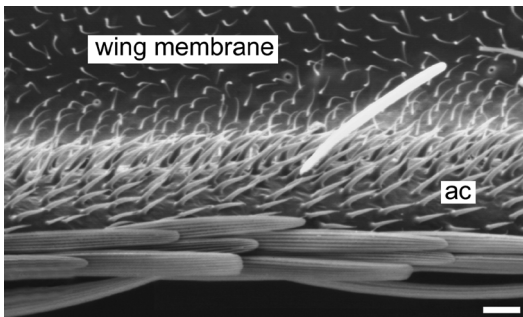


Fig. 47. SEM of the left forewing ambient costa of *Ceraclea* sp. (Leptoceridae), ventral view. Scale bar = 10 μ m.

opposite the forewing patches of setae. Arising from the basal region to approximately half the length of subcosta is a “tuft” of greatly elongated and comparatively slender setae (Figs. 42 and 43); possibly this row becomes entangled in the forewing anal cell microtrichia during coupling.

LEPTOCERIDAE

The morphology of the WCA in Leptoceridae is

strikingly consistent and is a putative synapomorphy for the family. Examination of a series of taxa from the two subfamilies Triplectidinae and Leptocerinae revealed no significant differences in either the morphology of the individual components or their distribution. The general structure of the apparatus is strikingly analogous to that of the hamular system of Hymenoptera, a similarity noted by Tillyard (1918) and sufficient for him to suggest the term “multihammulate.” In a survey of the wing scales and setae of the leptocerid *Pseudoleptocerus chirindensis* Kimmins, Huxley and Barnard (1988) identified and described the four putative coupling components.

As with Calamoceratidae and Odontoceridae, there is a well-defined patch of microtrichia confined to the posterior region of the anal angle, which continues along ambient costa until it terminates at the insertion of Cu2 (Figs. 44–48), and which results in a much more robust structure that projects slightly from the plane of the wing. The microtrichia in the anal angle are long and acuminate, but become comparatively shorter and slightly sinusoidal distally along ambient costa (Fig. 48); A1+2+3 is closely approximate

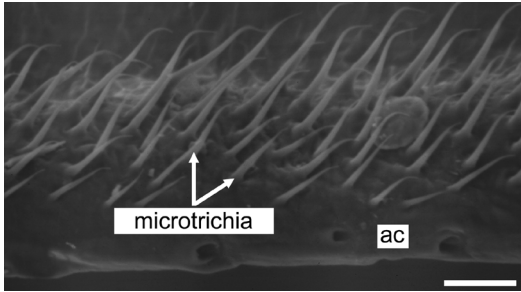


Fig. 48. SEM of the left forewing ambient costa of *Mystacides sepulchralis* (Walker) (Leptoceridae), ventral view. Scale bar = 10 μ m.

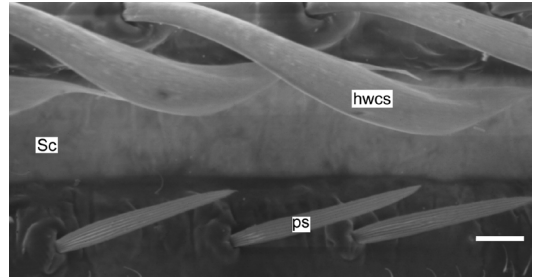


Fig. 49. SEM of the right hindwing coupling setae of *Oecetis avara* (Banks) (Leptoceridae), dorsal view. Scale bar = 10 μ m.

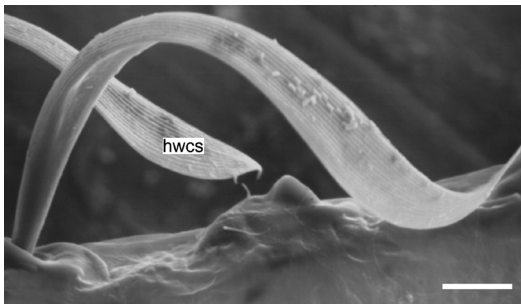


Fig. 50. SEM of the right hindwing coupling setae of *Setodes* sp. (Leptoceridae), dorsal view. Scale bar = 10 μ m.

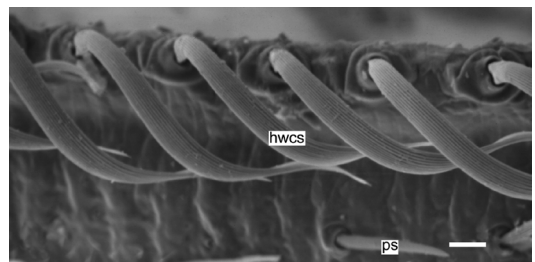


Fig. 51. SEM of the right hindwing coupling setae of *Mystacides sepulchralis* (Walker) (Leptoceridae), dorsal view. Scale bar = 10 μ m.

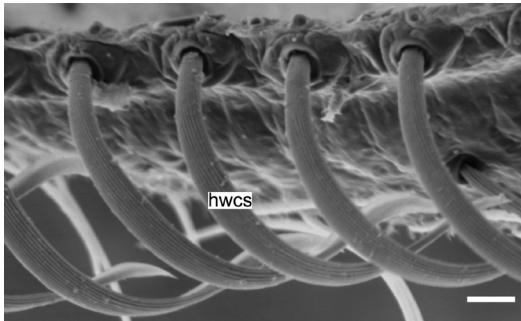


Fig. 52. SEM of the right hindwing coupling setae of *Oecetis avara* (Banks) (Leptoceridae), dorsal view. Scale bar = 5 μ m.

to ambient costa for its entire length, which may contribute to the rigidity of the hind margin of the wing.

The hindwing coupling apparatus consists of the coupling setae (hamular scales of Huxley & Barnard 1988) located on costa, and two other morphologically distinct setal types that are putatively part of the coupling apparatus. The

coupling setae (hindwing coupling setae, hwcs) are restricted to a morphologically well-defined region on costa that is somewhat variable in extent among taxa (Figs. 49–52). The setae are evenly spaced, arise from distinct mammae-like sockets, and are circular in cross-section basally, but become progressively more compressed in cross section prior to narrowing at the tip. Each seta projects away from costa and assumes a distally directed sinusoidal shape. In the region of the coupling setae, subcosta is closely approximate to costa and slightly dorsally impressed. The row of coupling setae along costa assumes a ledge-like form that projects dorsally from costa, and opposing this ledge is a second row of setae that arise from subcosta. Termed peg-like setae (ps) by Huxley and Barnard (1988), these project away from the membrane and are oriented distally; between this row of setae and the coupling setae the wing membrane is glabrous (Figs. 49 and 51). Huxley and Barnard (1988) speculated that the peg-like setae were involved in the coupling apparatus, perhaps as proprioceptive setae.

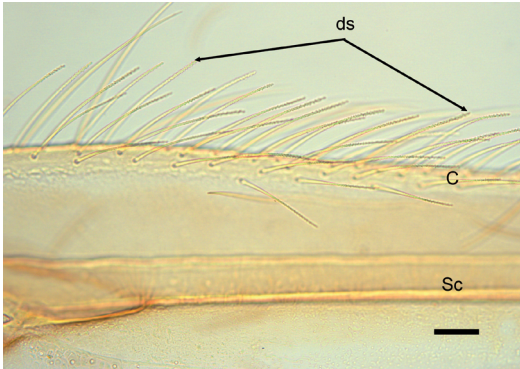


Fig. 53. LM of the basal right hindwing of *Ceraclea tarsipunctata* (Vorhies) (Leptoceridae), with denticulate and costal setae, dorsal view. Scale bar = 100 μ m.

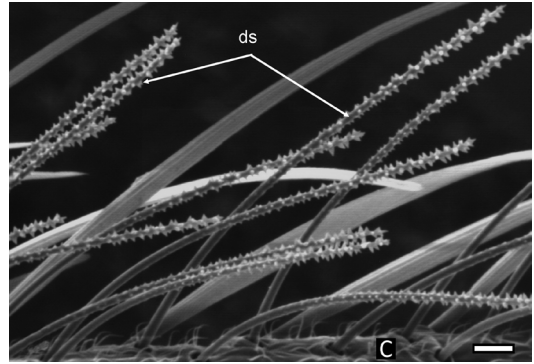


Fig. 54. SEM of the basal right hindwing denticulate setae of *Ceraclea* sp. (Leptoceridae), dorsal view. Scale bar = 10 μ m.

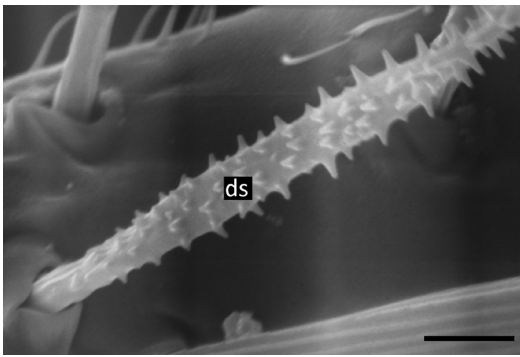


Fig. 55. SEM of the basal right hindwing denticulate setae *Nectopsyche* sp. (Leptoceridae), dorsal view. Scale bar = 5 μ m.

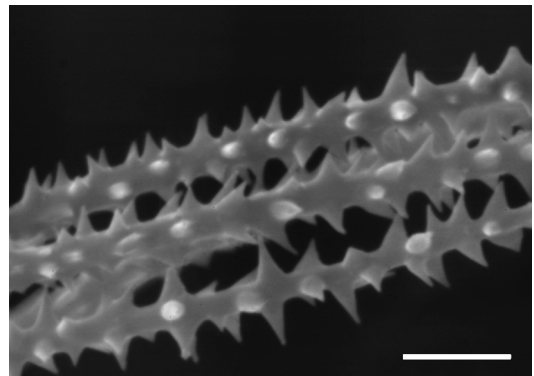


Fig. 56. SEM of the basal right hindwing denticulate setae of *Oecetis avara* (Banks) (Leptoceridae), dorsal view. Scale bar = 5 μ m.

Arising from the basal section of costa is a distinct class of setae that vary among taxa in their extent along costa. These long, slender and tapering setae were termed denticulate hairs by Huxley and Barnard (1988), who inferred a wing coupling function for these setae. The denticulate setae (ds) are remarkable for the shape of their dense denticles, where the length of a single denticle may exceed the diameter of the shaft (Figs. 53–56). I agree with Huxley and Barnard (1988) that these become embedded in the microtrichia in the anatomically opposite forewing anal angle region. While this may not contribute to the mechanical strength of the coupling system, it may serve to close the gap that is created in the axillary region when the wings are coupled; such a gap may have negative aerodynamic properties if it causes airflow to become disrupted. I further

agree that the biomechanical model suggested by the morphology is that the “[...] comb of hooked scales [...] clips on to the undercurled posterior edge of the forewing, possibly aided by the proprioceptive action of the row of peg-like setae that are immediately posterior to the tips of these scales” (Huxley & Barnard 1988).

MOLANNIDAE

Molannidae currently contains two valid genera, *Molannodes* McLachlan and *Molanna* Curtis, both of which have a WCA. The apparatus of *Molanna* was investigated and that of *Molannodes* (as *Indomolannodes*) figured and was briefly described by Wiggins (1968) as “[...] typical for the family”. If the morphology of

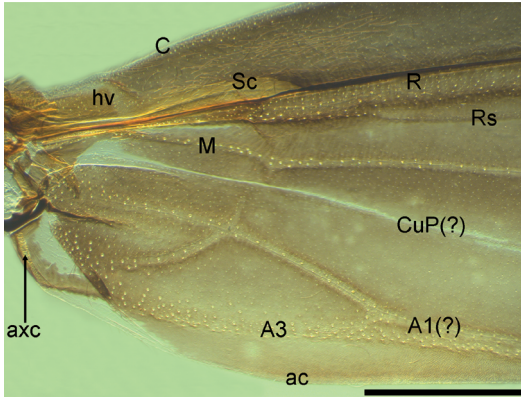


Fig. 57. LM of the left forewing of *Molanna ulmerina* Navás (Molannidae), anal angle region, ventral view. Scale bar = 1 mm.

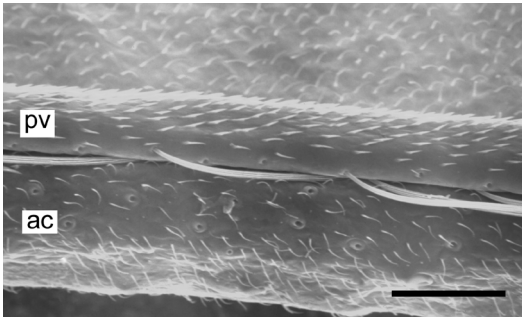


Fig. 59. SEM of the left forewing ambient costa and pseudovein of *Molanna ulmerina* Navás (Molannidae), ventral view. Scale bar = 50 μ m.

the WCA components in *Molannodes* is indeed consistent with that of *Molanna*, it may be a family-level synapomorphy. Biomechanically the apparatus is closely analogous to the hamular system of Hymenoptera, relying on recurved setae on the hindwing costa and a reinforced trough-like structure on the forewing. The system is also remarkably similar in morphological details to that of Helicopsychidae, which is discussed below. In *Molanna ulmerina* (Navás), the forewing venation is highly modified and difficult to interpret, leading to equivocation regarding some vein homologies, especially Cu2 and the anal veins. Evident in mounted wings and in SEM images is that the forewing coupling groove is structurally complex and involves three anatomical components: ambient costa, which is displaced ventrally from the plane of

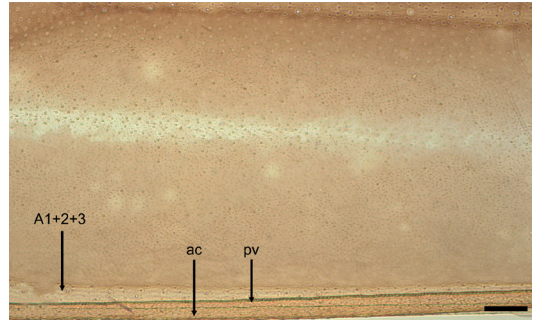


Fig. 58. LM of the left forewing of *Molanna ulmerina* Navás (Molannidae), ventral view. Scale bar = 100 μ m.

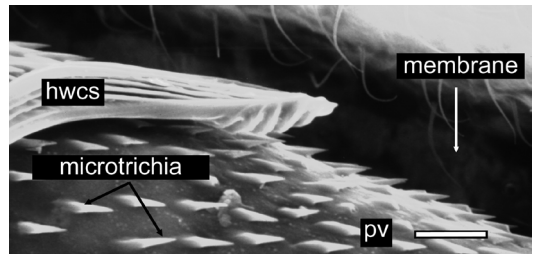


Fig. 60. SEM of the right hindwing coupling seta of *Molanna ulmerina* Navás (Molannidae) engaged on forewing pseudovein, dorsal view. Scale bar = 10 μ m.

the wing, a pseudovein (cuticular neoformation) immediately adjacent to ambient costa, and A1+2+3, which is separated from the previous two structures by a narrow space such that there is effectively no anal cell (Figs. 57–59). The surface of the pseudovein is markedly adorned with distally projecting microtrichia that serve to grip the hindwing coupling setae (Figs. 59 and 60). The anal angle is also adorned with acuminate microtrichia which continue onto both ambient costa and the pseudovein (Fig. 57).

The hindwing coupling setae are modified setae that assume a profile similar to those of Leptoceridae and Helicopsychidae. Strongly fluted shafts emerge from evenly spaced pronounced sockets on the dorsal surface of costa for approximately the basal half of costa (Fig. 61). Basally on costa the coupling setae are more widely spaced, but the coupling setae become more densely spaced in roughly the middle third of costa. The setae are longitudinally fluted but assume a twist that imparts a spiral contour to the flutes; distally the apex is tapered (Figs. 62

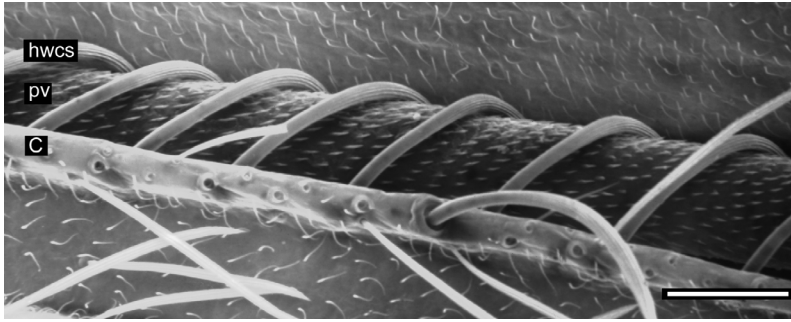


Fig. 61. SEM of the left engaged coupling mechanism of *Molanna ulmerina* Navás (Molannidae), ventral view. Scale bar = 10 μ m.

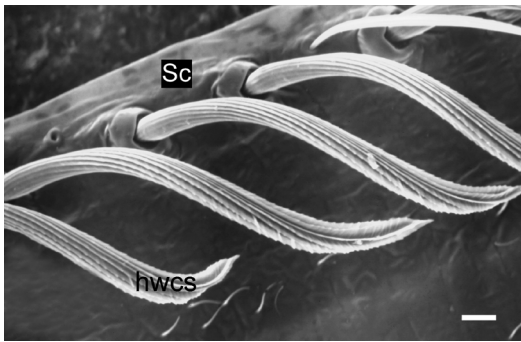


Fig. 62. SEM of the right hindwing coupling setae of *Molanna ulmerina* Navás (Molannidae), dorsal view. Scale bar = 10 μ m.

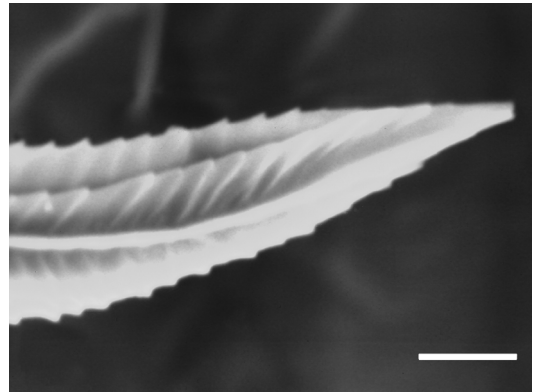


Fig. 63. SEM of the apex of a hindwing coupling seta of *Molanna ulmerina* Navás (Molannidae). Scale bar = 10 μ m.

and 63). The radius of curvature of the row of setae, as evidenced by SEM images of wings with the WCA engaged, matches the radius of curvature of the forewing pseudovein that they engage (Fig. 61). In this position, the microtrichia that cover the pseudovein can engage the serrated flutes of the coupling setae; presumably this prevents excessive slippage of the apparatus when engaged.

Sericostomatoidea

The family-level phylogeny of Sericostomatoidea is uneven, with 579 described species (Holzenthal *et al.* 2007b, Morse 2009) in twelve families; only the two cosmopolitan families Helicopsychidae and Sericostomatidae contain more than one hundred species each. The monophyly of the superfamily is recovered with strong support but there is no support for any family-level relationships except a Hydrosalp-

ingidae + Petrothrincidae sister-taxon relationship (Holzenthal *et al.* 2007b).

SERICOSTOMATIDAE

The taxonomic history of Sericostomatidae has been turbulent, which is not surprising since it one of the oldest Trichoptera families, and has traditionally been a “dumping ground for genera unable to be placed with confidence in other families” (Holzenthal *et al.* 2007b); as currently construed it is probably paraphyletic (Holzenthal *et al.* 2007a). The taxa *Gumaga* Tsuda, *Sericostoma* Latreille and *Agarodes* Banks are recovered as a weakly supported monophylum by Holzenthal *et al.* (2007b) in molecular analyses, but currently no morphological characters are known that support the monophyly of the family.

The WCA of the species *Agarodes tetron* (Ross) and *Fattigia pele* (Ross) are morphologi-

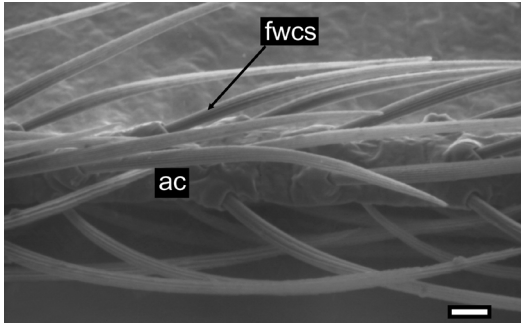


Fig. 64. SEM of the left forewing coupling setae of *Agarodes libalis* Ross & Scott (Sericostomatidae), ventral view. Scale bar = 10 μm .

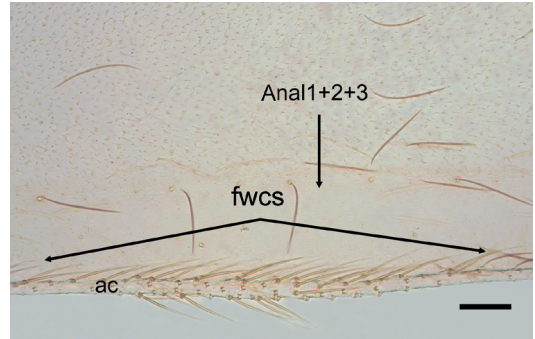


Fig. 65. LM of the left forewing coupling setae of *Fattigia pele* (Ross) (Sericostomatidae), ventral view. Scale bar = 100 μm .

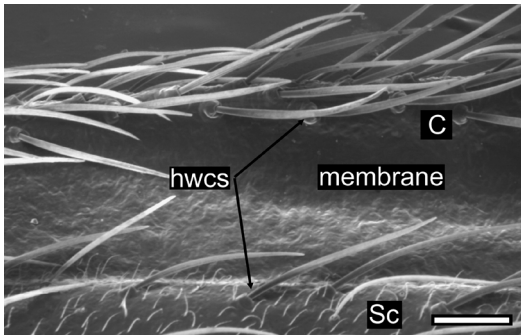


Fig. 66. SEM of the right hindwing coupling setae of *Agarodes libalis* Ross & Scott (Sericostomatidae), dorsal view. Scale bar = 50 μm .

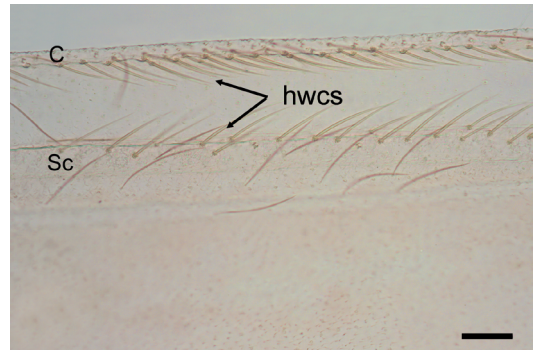


Fig. 67. LM of the right hindwing coupling setae of *Fattigia pele* (Ross) (Sericostomatidae), dorsal view. Scale bar = 100 μm .

cally similar and may, if additional genera are studied, serve as a synapomorphy for some clade of sericostomatid genera. The forewing has a bed of microtrichia on the ventral anal angle which is sometimes restricted to ambient costa and which reinforces the posterior margin of the forewing. Beginning at approximately the mid-length of the posterior margin is a well-defined group of apically projecting socketed setae, which encircle the posterior and ventral surfaces of the vein (Figs. 64 and 65). The coupling setae, which project away from the vein at $\sim 30^\circ$ – 45° and are slightly serrate at their apices, continue for $\sim 15\%$ the length of the posterior margin, after which the morphology of the setae changes abruptly to typical vein-covering setae. The hindwing component of the WCA is composed of two opposing fields of socketed setae on the dorsal aspect in a position anatomically opposite the forewing setal cluster (Figs. 65 and 67). The setae arise

from both costa and subcosta and are directed apically at $\sim 45^\circ$. Topologically the coupling region is defined anteriorly by the circumferential brush of coupling setae along costa, posteriorly by an opposing row of linearly arranged setae, and dorsally by a region of membrane; this topology creates a seta-bordered trough which engages the forewing coupling setae.

HELICOPSYCHIDAE

Wing coupling structures in Helicopsychoidea are illustrated in the Trichoptera literature, and Johanson (1998), using SEM, examined and illustrated the coupling setae of *Helicopsyche boulearia* Ross. The coupling setae, which vary in number among taxa, are inserted in deep sockets along the dorsal margin of costa. The

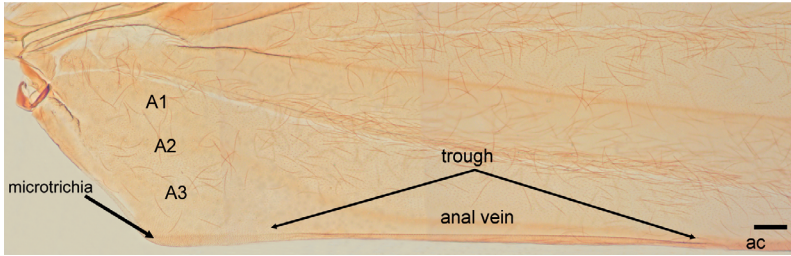


Fig. 68. LM of the left forewing of *Helicopsyche limnella* Ross (Helicopsychidae), showing trough, ventral view. Scale bar = 100 μ m.

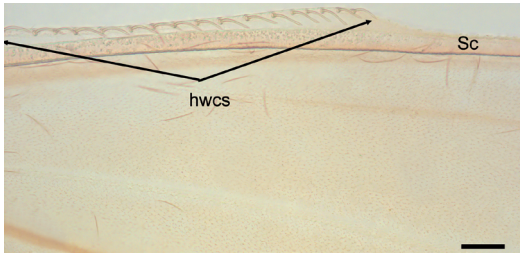


Fig. 69. LM of the right hindwing coupling setae of *Helicopsyche limnella* Ross (Helicopsychidae), dorsal view. Scale bar = 100 μ m.

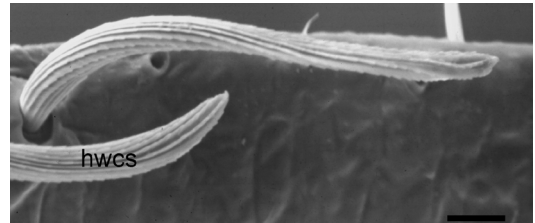


Fig. 70. SEM of the right hindwing coupling setae of *Helicopsyche borealis* (Hagen) (Helicopsychidae), dorsal view. Scale bar = 10 μ m.

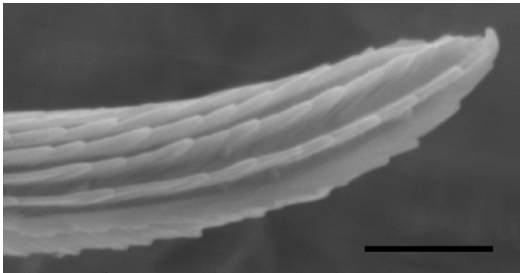


Fig. 71. SEM of the apex of a hindwing coupling seta of *Helicopsyche borealis* (Hagen) (Helicopsychidae). Scale bar = 5 μ m.

coupling setae display morphological consistency both within a single individual and among taxa, and are modified fluted setae (Figs. 68–71) that assume an axial twist in the shaft. The row of coupling setae is arranged such that they project dorsally from the plane of the hindwing, and such that they acquire a distally projecting orientation; the change in orientation is due to the presence of a smooth bend in the setal shaft (Fig. 70). The coupling setae engage the ambient costal vein that is shifted away from the plane of the wing membrane. This shift results in a trough-like structure composed of the ambient costa (Fig. 68), which is adorned with distally projected microtrichia, the closely approximate

A1+2+3, and the membrane between ambient costa and A1+2+3. Examination suggests that the coupling system is a synapomorphy for Helicopsychidae.

CHATHAMIIDAE, CALOCIDAE, CONOESUCIDAE AND HELICOPHIDAE

The species *Philanisus plebeius* Walker (Chathamidae), *Alloecentrella magnicornis* Wise (Calocidae), *Beraeoptera roria* Mosely (Conoesucidae) and *Zelolessica cheira* McFarlane (Helicophidae) were examined. These families are placed in Sericostomatoidea with strong support (Holzenthal *et al.* 2007a), but the interfamilial relationships are unclear. In *P. plebeius* the forewing component of the WCA is comprised of two subunits, and at least superficially it is structurally similar to that of Molannidae (Fig. 72). Ambient costa is reflexed ventrally, thickened, and adorned with a dense bed of acuminate microtrichia (Fig. 72). Immediately distal to the anal angle and approximate to A3 is a region of sclerotized cuticle that forms a pseudovein. The pseudovein increases in diameter as it becomes approximate to ambient costa in the middle of the wing margin, and disappears proximal to

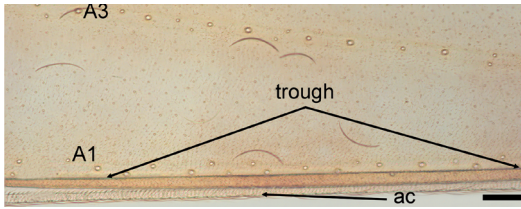


Fig. 72. LM of the left forewing of *Philanisus plebeius* Walker (Chathamidae), showing trough, ventral view. Scale bar = 100 μ m.

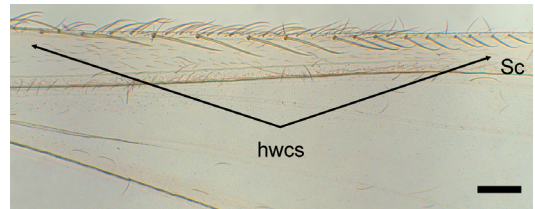


Fig. 73. LM of the right hindwing coupling setae of *Philanisus plebeius* Walker (Chathamidae), dorsal view. Scale bar = 100 μ m.

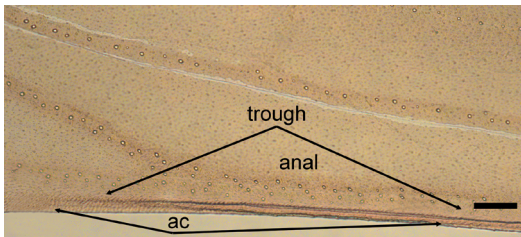


Fig. 74. LM of the left forewing of *Alloecentrella magnicornis* Wise (Calocidae), showing trough, ventral view. Scale bar = 100 μ m.

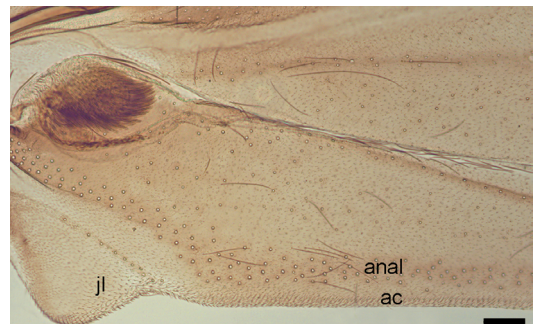


Fig. 75. LM of the left forewing of *Beraeoptera roria* Mosely (Conoesucidae), ventral view. Scale bar = 100 μ m.

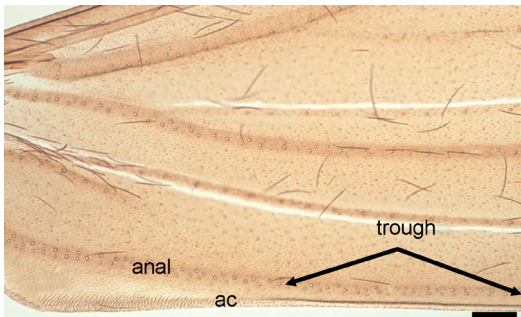


Fig. 76. LM of the left forewing of *Zelolessica cheira* McFarlane (Helicophidae), showing trough, ventral view. Scale bar = 1 mm.

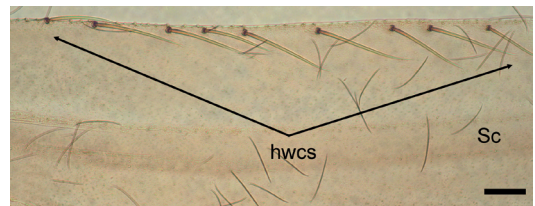


Fig. 77. LM of the right hindwing coupling setae of *Alloecentrella magnicornis* Wise (Calocidae), dorsal view. Scale bar = 100 μ m.

the insertion of A1+2 on the wing margin. Thus, the ambient costa and the pseudovein form the posterior edge of a ventral trough-like structure (Fig. 72; trough) bounded dorsally by the wing membrane and anteriorly by a closely approximate A1+2.

The hindwing component of the WCA is comprised of a linear series of costal setae that project dorsally and apically from costa (Fig. 73). Basally on costa the setae are more or less straight, but distally the setae are relatively shorter and each assumes a curved profile towards the tip. Presumably these setae engage

the forewing by hooking over and into the ventral trough on the forewing posterior margin.

A similar apparatus is present in *A. magnicornis* (Fig. 74), *B. roria* (Fig. 75) and *Z. cheira* (Fig. 76), which differ primarily in that the posteroventral margin of the forewing coupling trough is composed of ambient costa only; while the margin is clearly reinforced, no additional pseudovein can be discerned (Figs. 74–76). In general shape and distribution, the hindwing costal setae of *P. plebeius* are similar to those of *A. magnicornis* (Fig. 77). The costal setae of *Z. cheira* differ further by being more widely spaced, evenly sized, and each evenly curved to

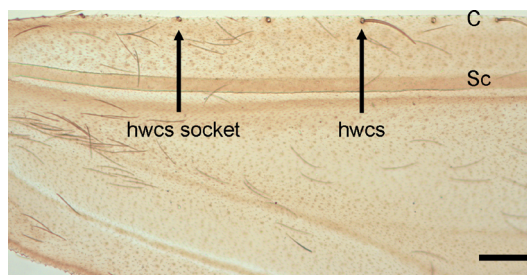


Fig. 78. LM of the right hindwing coupling setae of *Zelolessica cheira* McFarlane (Helicophidae), dorsal view. Scale bar = 1 mm.



Fig. 79. LM of the right hindwing coupling setae and costa of *Beraeoptera roria* Mosely (Conoesucidae), dorsal view. Scale bar = 1 mm.

a tapered tip without a pronounced distal curvature (Fig. 78). The costal setae in *B. roria* are reduced even further and attached only weakly, but the costal margin is considerably more robust (Fig. 79). In this species costa protrudes dorsally, has a wider diameter and is adorned, like ambient costa of the forewing, with acuminate, apically directed, microtrichia. The interaction model suggested by this conformation is different from that of the other taxa, in that the dorsally projecting lip of the hindwing engages with the ventrally projecting lip of the forewing; the costal setae may participate, but the primary interaction appears to be due to the opposing and intermeshing fields of microtrichia.

Integripalpia: Plenitentoria

No suprafamilial plenitentorian taxa are supported in combined analyses, but the superfamily “Limnephiloidea”, comprising nine of the thirteen families, is conventionally recognized (e.g., Vshivkova *et al.* 2006). The cosmopolitan family Limnephilidae *sensu lato* comprises 1204 of the 1924 species in Plenitentoria, but Limnephilidae *sensu lato* (806 species) is typically broken into the five families Apataniidae (197 species), Goeridae (169 species), Limnephilidae *sensu stricto* (806 species), Rossianidae (2 species) and Uenoidae (30 species; Morse 2003, 2009). Holzenthal *et al.* (2007a) failed to find support for intrafamilial arrangements in Limnephiloidea, but there was strong support for a monophylum comprised of the above five families. Vshivkova *et al.* (2006) provided strong morphological support for a monophyletic Lim-

nephilidae. A number of traditional plenitentorian families were supported in combined analyses (Holzenthal *et al.* 2007a), including Brachycentridae, Phryganaeidae, Pisuliidae, Oeconesidae, and Lepidostomatidae.

Oeconesidae

Examination of the wings of *Pseudoeconesus bistirpis* Wise, *P. hudsoni* Mosely and *Oeconesus maori* McLachlan support the analysis of Holzenthal *et al.* (2007a) that these taxa form a monophylum. No data are available regarding the flight dynamics of Oeconesidae but the morphology of the wings suggests that they do couple their wings for an entire beat cycle, even though *in vitro* manipulations did not produce a convincing interaction. The jugal lobe of *P. hudsoni* is smaller and less protrusive than in Phryganaeidae, and the jugal lobe of *O. maori* is virtually absent. The anal cell is rather wide, as in Phryganaeidae, but is populated with relatively more robust socketed setae; ambient costa is not reinforced and possesses microtrichia and setae typical of the general wing vestiture (Fig. 80).

The hindwing of *P. bistirpis*, which is similar to that of *P. hudsoni*, has greatly enlarged setae that begin in the prehumeral area, but in this species the humeral vein is either absent or inconspicuous; the setae, which are elongate basally, rapidly decline in length until they are absent distal to the basal quarter of the wing length (Fig. 81). The hindwing setae of *O. maori* are similarly difficult to divide into prehumeral and costal groups. The prehumeral vein is discernible but inserts on costa after deviating from the



Fig. 80. LM of the left forewing of *Pseudoeconesus hudsoni* Mosely (Oeconesidae), ventral view. Scale bar = 1 mm.

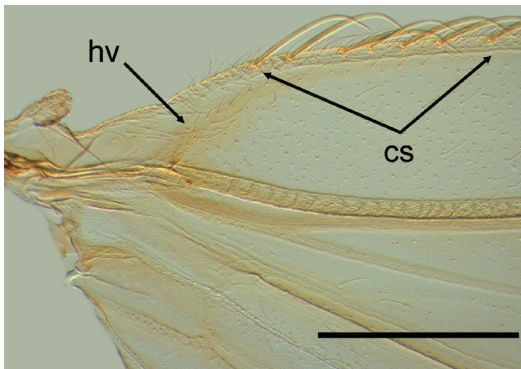


Fig. 82. LM of the right hindwing of *Oeconesus maori* McLachlan (Oeconesidae), dorsal view. Scale bar = 1 mm.

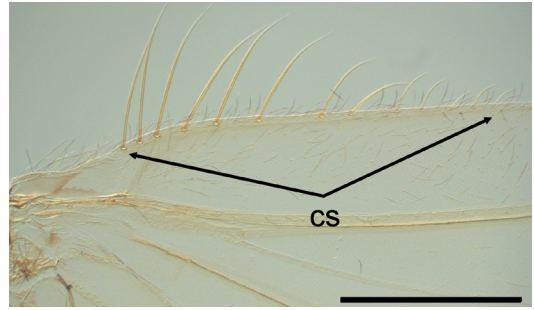


Fig. 81. LM of the right hindwing of *Pseudoeconesus bistirpis* Wise (Oeconesidae), dorsal view. Scale bar = 1 mm.

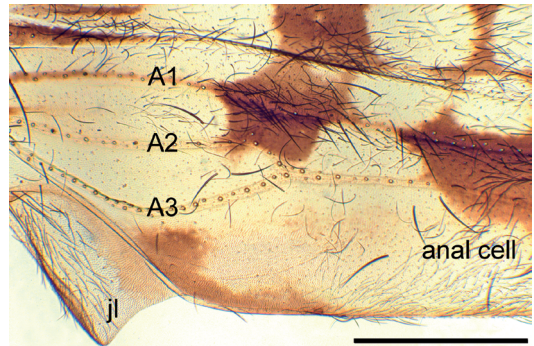


Fig. 83. LM of the left forewing of *Banksiola dossuaria* (Say) (Phryganeidae), ventral view. Scale bar = 1 mm.

typical course and becoming parallel to costa; these groups of setae, which are also morphologically indistinguishable, may represent the costal setae only (Fig. 82). The setae are, however, more robust than those of *P. hudsoni*, shorter and more distinctly curved. The row is more nearly uniform in length, but diminishes quickly after the basal third of the wing length.

Phryganeidae

Previous flight experiments demonstrated that *Semblis atrata* (Gmelin) did not fly with coupled wings (Ivanov 1991). However, the morphology of the forewing jugal lobe and the hindwing prehumeral setae suggests strongly that these

are engaged during the down stroke in a manner similar to that of *Parapsyche* sp. (Hydropsychidae: Annulipalpia) and *Phylocentropus* sp. (Dipseudopsidae: Annulipalpia) (author's unpubl. data). In *Banksiola dossuaria* (Say) the jugal lobe is well developed with a reinforced margin that is produced slightly ventrad. Both the jugal lobe and the anal angle of the anal cell are clothed in microtrichia, which in the anal angle region is represented by two discrete classes of microtrichia, an inner region of short, recurved spinose projections, surrounded by a field of more elongate and tapered spines typical of the general covering microtrichia (Figs. 83 and 84). As in *Parapsyche* sp. and *Phylocentropus* sp. the anal cell is quite wide. The microtrichia may have a functional role in wing coupling, but may have a more dominant role in keeping the forewings locked together while in the tectiform position.

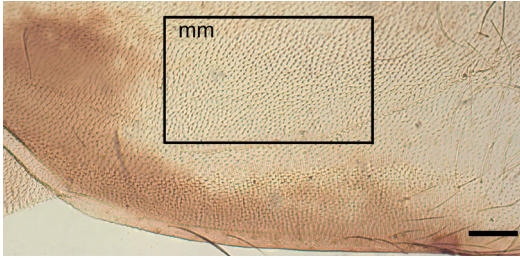


Fig. 84. LM of basal region of the left forewing *Banksiola dossuaria* (Say) (Phryganaeidae), ventral view. Boxed region mm = major microtrichia. Scale bar = 100 μ m.

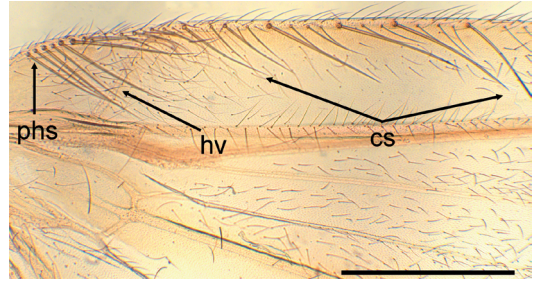


Fig. 85. LM of prehumeral setae and costal setae of the right hindwing of *Banksiola dossuaria* (Say) (Phryganaeidae), dorsal view. Scale bar = 1 mm.

The hindwing prehumeral setae are present as a linear row on the dorsal aspect of costa and are simply elongated and enlarged fluted setae. The costal setae are morphologically similar to the prehumeral setae but are more widely spaced; other than the presence of the humeral vein that divides the two groups of setae, no morphological criterion for discriminating between prehumeral and costal setae is apparent (Fig. 85). In general morphology the setae strongly resemble the prehumeral and costal setae of Limnephilidae *sensu stricto*. Again, these may engage in some manner the forewing while in flight, but no such interaction could be reproduced *in vitro*.

BRACHYCENTRIDAE

Wing coupling was observed with high speed cinematography in *Micrasema* sp. (author's unpubl. data). Although a sister taxon relationship between *Micrasema* McLachlan and *Brachycentrus* Curtis was not recovered with strong support by Holzenthal *et al.* (2007a), the WCA of these two taxa is morphologically uniform. The forewing has a discernable jugal lobe and the ambient costa is adorned with greatly elongate socketed setae that are recumbent along ambient costa in an apical orientation; ambient costa is noticeably reinforced and the anal veins are close and parallel (Figs. 86–88). The anal cell

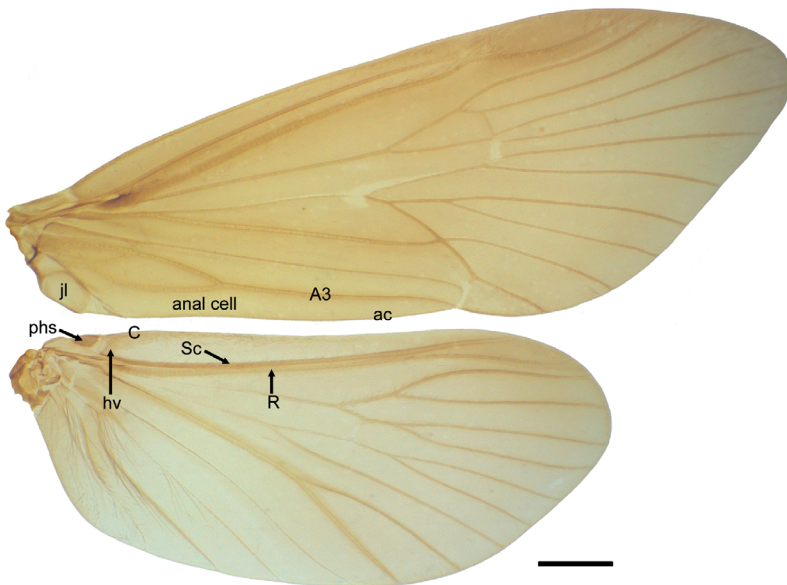


Fig. 86. LM of right fore- and hindwings of *Brachycentrus* sp. (Brachycentridae), dorsal view. Scale bar = 1 mm.

Fig. 87. LM of right fore- and hindwings of *Micrasema* sp. (Brachycentridae), dorsal view. Scale bar = 1 mm. Boxed area A indicates the interaction area of the forewing jugal lobe and the hindwing prehumeral setae. Boxed area B indicates the interaction area between the coupling setae of the forewing ambient costa and hindwing costa.

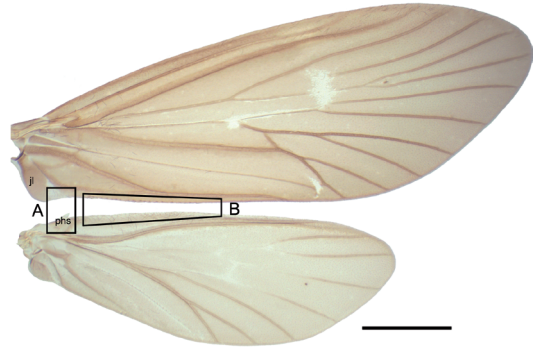


Fig. 88. LM of ventral surface of left forewing of *Micrasema* sp. (Brachycentridae), ventral view. Scale bar = 0.5 mm.

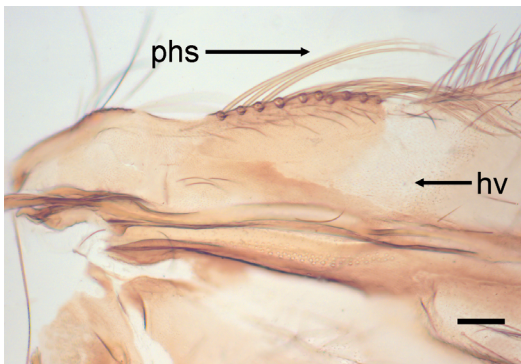
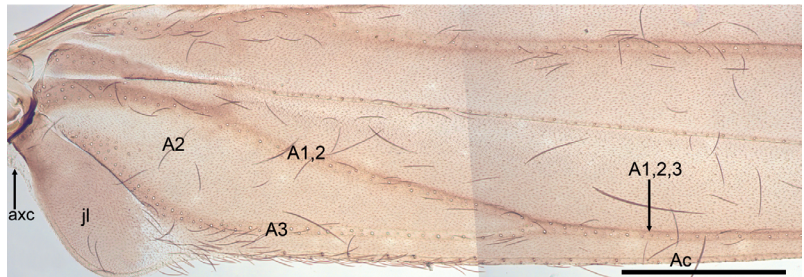


Fig. 89. LM of right hindwing prehumeral setae of *Brachycentrus* sp. (Brachycentridae), dorsal view. Scale bar = 100 μm .

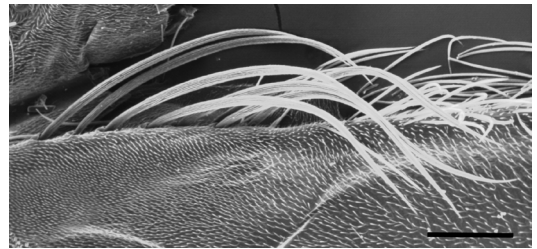


Fig. 90. SEM of right hindwing prehumeral setae of *Brachycentrus* sp. (Brachycentridae), dorsal view. Scale bar = 100 μm .

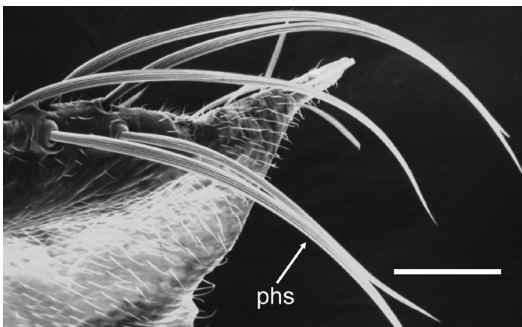


Fig. 91. SEM of right hindwing prehumeral setae of *Brachycentrus* sp. (Brachycentridae), dorsal view. Scale bar = 100 μm .

in *Micrasema* sp. is very narrow, and slightly wider in *Brachycentrus* sp., but in both taxa the margins of the forewing and hindwing are parallel (Figs. 86 and 87). Topologically the recumbent setae of the forewing are displaced ventrally from the plane of the wing such that they form a circumferential brush of setae.

In the hindwing, a prominent linear row of tapering setae is basal to the humeral vein (Figs. 89–92), distal to which is a row of distinctive setae that project dorsally, obliquely and apically. The setae are straight and possess teeth that arise from the serrations along the longitudinal carinae that define the flutes of the setal shaft (Figs. 93 and 94). The morphology of the system suggests the following biomechanical

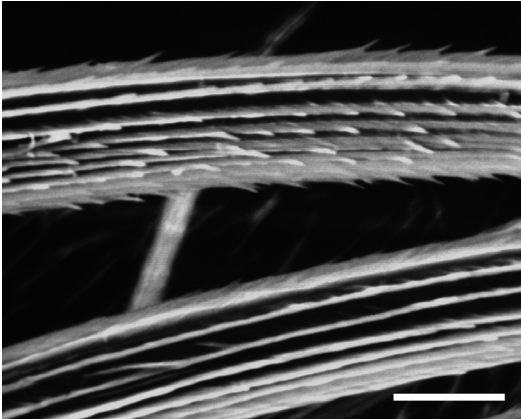


Fig. 92. SEM of right hindwing prehumeral setae of *Micrasema* sp. (Brachycentridae), dorsal view. Scale bar = 50 μ m.



Fig. 94. SEM of right hindwing coupling setae of *Micrasema* sp. (Brachycentridae), dorsal view. Scale bar = 10 μ m.

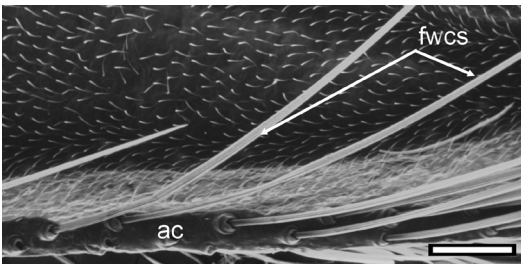


Fig. 96. SEM of left forewing coupling setae of *Micrasema* sp. (Brachycentridae), ventral view. Scale bar = 50 μ m.

model: The hindwing costal setae, which project dorsally, become entangled and embedded in the circumferential brush of elongate and recumbent setae on the ventral aspect of forewing ambient costa (Figs. 95 and 96). The interaction does not engage in a precise manner, but instead relies on a “probabilistic” interaction described for other locking mechanisms, as discussed by Gorb *et al.* (2002).

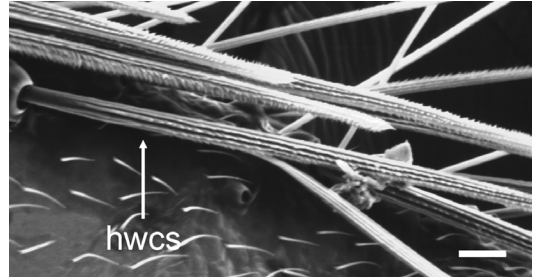


Fig. 93. SEM of right hindwing coupling of *Micrasema* sp. (Brachycentridae), dorsal view. Scale bar = 10 μ m.

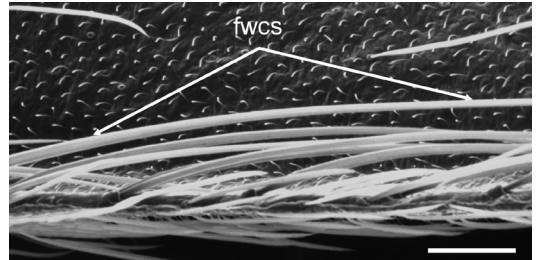


Fig. 95. SEM of left forewing coupling setae of *Micrasema* sp. (Brachycentridae), ventral view. Scale bar = 50 μ m.

Lepidostomatidae

High speed cinematography of *Lepidostoma* sp. conclusively demonstrated that the forewings and hindwings are engaged on the down stroke only (author’s unpubl. data), enforced presumably by the interaction between the jugal lobe and prehumeral setae. The general morphology of the basal aspects of the down stroke WCA in *Lepidostoma* sp. and *Theliopsyche* sp. are similar to that of Brachycentridae, but the morphology of the wings in Lepidostomatidae is highly variable among species and between the sexes; the contour of the wings is highly variable (especially the posterior forewing margin), and the nature of the wing vestiture varies from simple setae to very complex scale-like setae. In *Lepidostoma togatum* (Hagen) the posterior margin of the forewing is parallel to the costal margin of the hindwing, and the anal cell is also quite narrow such that the anal vein is closely approximate to hindwing costa (Fig. 97); collectively these elements are consistent with wing coupling, but this was not observed or duplicated *in vitro*.

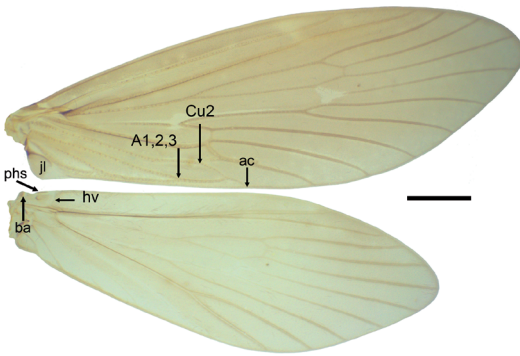


Fig. 97. LM of right forewing and hindwing of *Lepidostoma togatum* (Hagen) (Lepidostomatidae), dorsal view. Scale bar = 0.5 mm.



Fig. 98. LM of left forewing basal region of *Lepidostoma togatum* (Hagen) (Lepidostomatidae), ventral view. Scale bar = 0.5 mm.

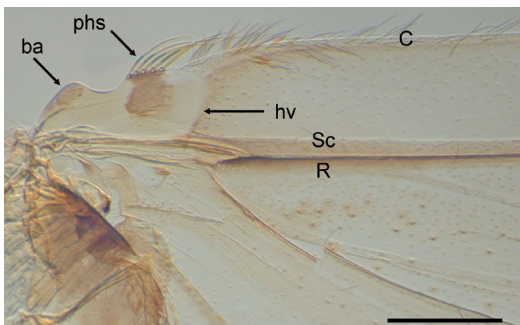


Fig. 99. LM of the right basal hindwing of *Lepidostoma togatum* (Hagen) (Lepidostomatidae), showing prehumeral setae and basal apophysis, dorsal view. Scale bar = 1 mm.

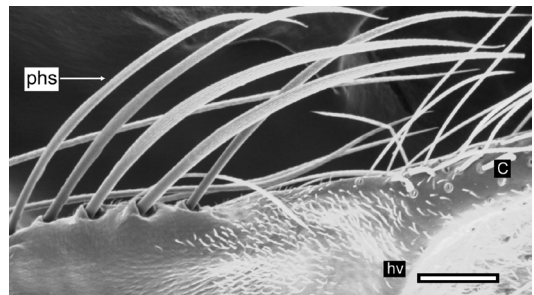


Fig. 100. SEM of the right basal hindwing prehumeral setae of *Lepidostoma togatum* (Hagen) (Lepidostomatidae), dorsal view. Scale bar = 50 μ m.

The forewing jugal lobe (Fig. 98) is similar in shape and extent of development to that of Brachycentridae, as are the hindwing prehumeral setae (Figs. 99 and 100). Hindwing costa is adorned with setae that are similar to the typical wing vestiture and only weakly attached to the membrane. The prehumeral area does, however, present a structure that may be valuable as a synapomorphy if observed in additional taxa. Immediately basal to the prehumeral bristles the margin assumes a pronounced declivity, the contour of which is made more pronounced by the enlarged lobe immediately basal to it (Fig. 99; basal apophysis). The declivity is devoid of setae, but the lobe, which is apparently more sclerotized than the declivity, bears weakly attached setae. In shape and position this struc-

ture is suggestive of the costal sclerite of Lepidoptera, but this is presumed to be a homoplasy. What role this structure performs in wing coupling is unknown.

Apataniidae, Goeridae, Limnephilidae *sensu stricto* and Uenoidae

Until recently the above taxa and Rossianidae were included in the family Limnephilidae *sensu lato*, but recent analyses suggest that these families are each monophyletic and that Limnephilidae *sensu stricto* is monophyletic with respect to the remaining families; further relationships are still unclear, and collectively they form an unresolved polytomy with a relimited Limnephilidae (Holzenthal *et al.* 2007a). The putative WCA of taxa in these families shows consistent overall morphology and may represent an underlying

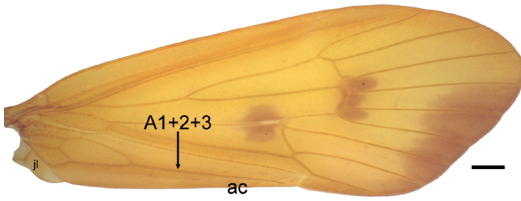


Fig. 101. LM of the left forewing of *Pycnopsyche sonso* Milne (Limnephilidae), ventral view. Scale bar = 1 mm.

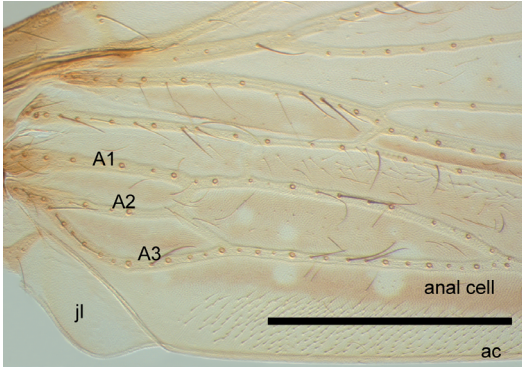


Fig. 103. LM of the anal angle region of the left forewing of *Glyphopsyche missouri* Ross (Limnephilidae), ventral view. Scale bar = 1 mm.

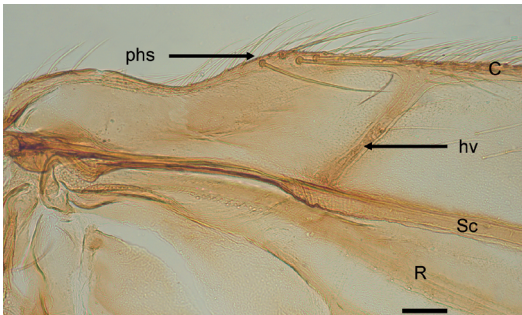


Fig. 105. LM of the right hindwing prehumeral setae and costal setae of *Chaetopteryx fusca* Brauer (Limnephilidae), dorsal view. Scale bar = 100 μ m.

form-functional theme onto which family and genus-level morphological variation has been added. The wing interaction mode is not known for any taxa in these families, but the anatomy of the wings strongly suggests that the wings are coupled during both the down-stroke and up-stroke.

In all taxa examined, there is evidence of a forewing jugal lobe (Figs. 101–103). The lobe

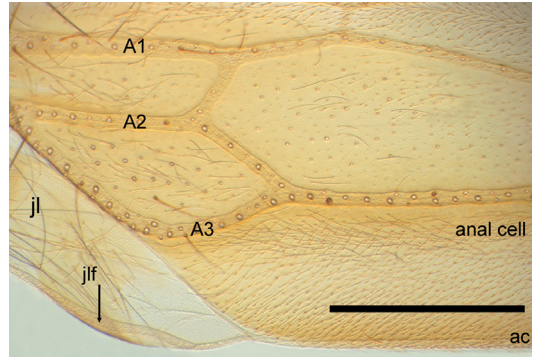


Fig. 102. LM of the anal angle region of the left forewing of *Pycnopsyche sonso* Milne (Limnephilidae), ventral view. Scale bar = 1 mm.

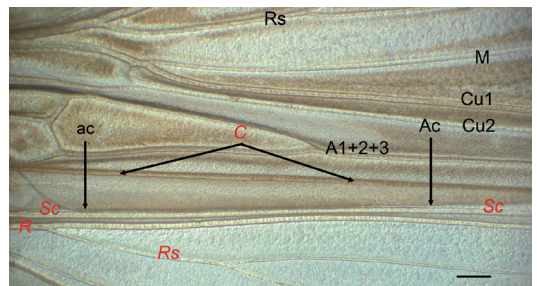


Fig. 104. LM of the right fore- and hindwing of *Hydatophylax argus* (Harris) (Limnephilidae), in the coupled position, dorsal view. Red italic letters indicate hindwing features. Scale bar = 1 mm.

in some taxa is somewhat diminished, but nonetheless retains a component that is putatively involved with engaging the hindwing prehumeral setae. Basally, ambient costa is a continuation of the axillary cord, which originates on the posterior notal process, and whose posterior margin defines the jugal lobe. A1+2+3 is typically close to ambient costa and parallel to it (Fig. 104). While the lobe itself is diminished, the highly extensible cord forms a ventrally recurved lip that defines a trough-like region that is ventrally open (Fig. 102: jlf); this trough presumably engages the hindwing prehumeral setae.

In the hindwings of all taxa examined there is a more or less prominent cluster of prehumeral setae (Figs. 105–114) that is basal to a pronounced humeral vein, distal to which costa is adorned with a circumferential brush of more or less developed setae. Taxonomically and possibly phylogenetically relevant variation is found

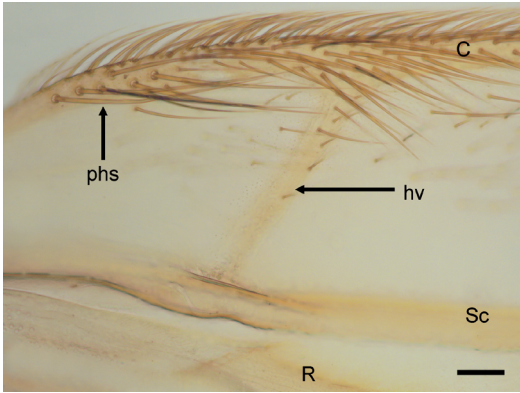


Fig. 106. LM of the right hindwing prehumeral setae and costal setae of *Pycnopsyche sonso* Milne (Limnephilidae), dorsal view. Scale bar = 100 μ m.

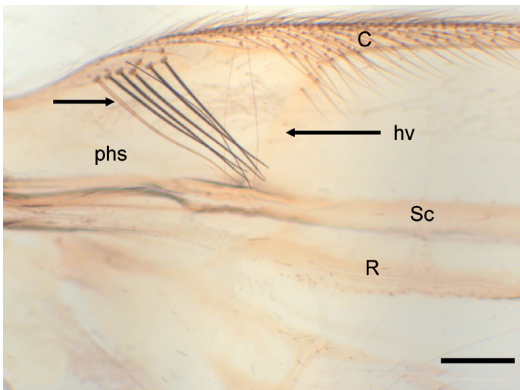


Fig. 108. LM of the right hindwing prehumeral setae and costal setae of *Hydatophylax argus* (Harris) (Limnephilidae), dorsal view. Scale bar = 1 mm.

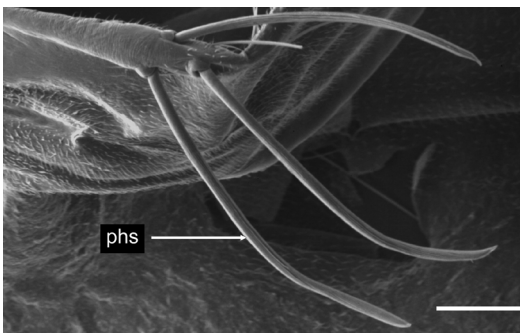


Fig. 110. SEM of the right hindwing prehumeral setae of *Apatania crymophila* McLachlan (Apataniidae), dorsal view. Scale bar = 100 μ m.

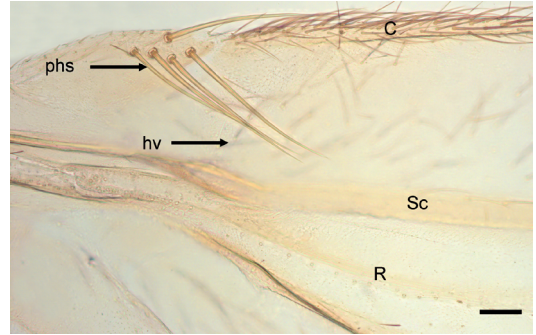


Fig. 107. LM of the right hindwing prehumeral setae and costal setae of *Ecclisomyia kamtschatica* (Martynov) (Limnephilidae), dorsal view. Scale bar = 100 μ m.

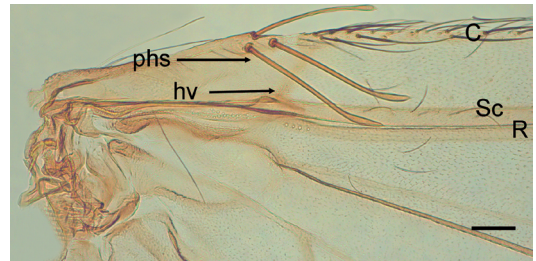


Fig. 109. LM of the right hindwing prehumeral and costal setae of *Apatania robusta* (Apataniidae), dorsal view. Scale bar = 100 μ m.



Fig. 111. LM of the right hindwing prehumeral and costal coupling setae of *Goera calcarata* Banks (Goeridae), dorsal view. Scale bar = 100 μ m.

ment setae arranged in an anatomically consistent position (Figs. 109 and 110). The setae are wide-diameter-fluted shafts that arise from pronounced sockets; the triad is ventrally and apically directed. Distally each shaft increases in diameter before tapering to a sharp tip, resulting in a conspicuously bulbous morphology distally. This morphology was observed in *Apatania* spp. and *Apataniana tschuktschorum* Levanidova and

in the development of the prehumeral setae. In *Apatania* sp. and *Apataniana* sp. (Apataniidae) the cluster is reduced to three promi-

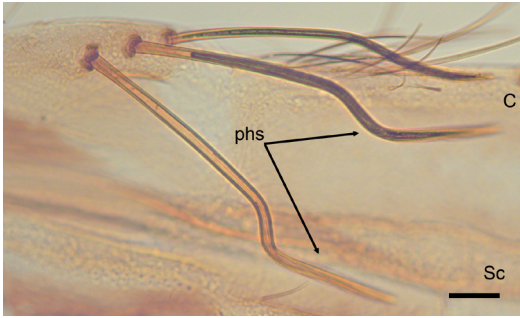


Fig. 112. LM of the right hindwing prehumeral setae of *Silo pallipes* (Fabricius) (Goeridae), dorsal view. Scale bar = 10 μ m.

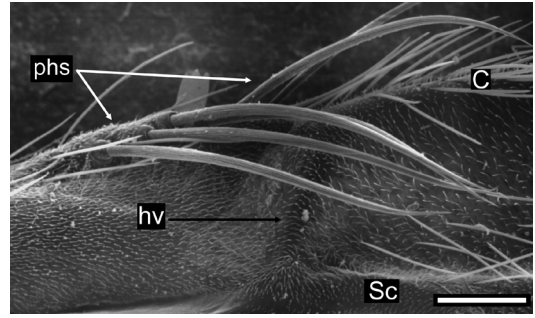


Fig. 113. SEM of the prehumeral setae of *Goera fuscula* Banks (Goeridae), dorsal view. Scale bar = 10 μ m.

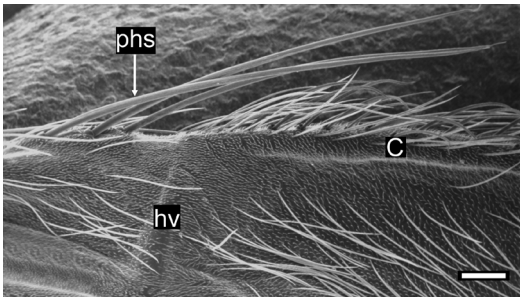


Fig. 114. SEM of right hindwing prehumeral and costal setae of *Neophylax ussuriensis* (Martynov) (Uenoidae), dorsal view. Scale bar = 100 μ m.

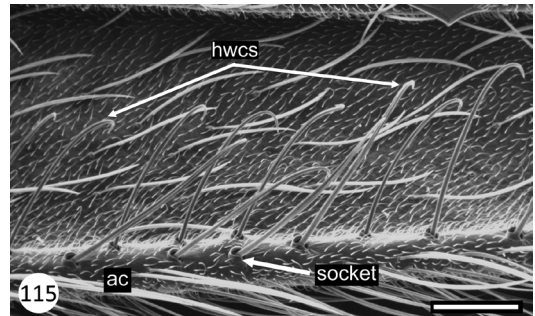


Fig. 115. SEM of right hindwing coupling setae of *Neophylax ussuriensis* (Martynov) (Uenoidae), dorsal view. Scale bar = 100 μ m.

may be a synapomorphy for these genera. In *Pedomoecus sierra* Ross (Fig. 111), *Allomyia gnathos* (Ross) and *Moselyana comosa* Denning the setae are simply tapered and in overall morphology are similar to those typical of Goeridae, Limnephilidae and Uenoidae.

The hindwing prehumeral setal cluster in Limnephilidae is variable in the extent of its development, but the morphology of the setae is uniform. In *Pycnopsyche sonso* Milne (Fig. 106), the cluster is diminished and the setae are undifferentiable from the remaining setae on the vein and are similar to the costal setae distal to the prehumeral vein. In *Chaetopteryx fusca* Brauer, *Ecclisomyia kamtschatica* (Martynov) and *Hydatophylax argus* (Harris), the cluster is well defined (Figs. 105, 107 and 108). The prehumeral setae in *Goera* spp. (Goeridae; Figs. 111 and 113) are similar to those of Limnephilidae, but with a tendency to be somewhat more elongate. In *Neophylax* spp. (Uenoidae;

Fig. 114) the three setae in the cluster are considerably more elongate and extend well beyond the prehumeral vein. The prehumeral setae of *Silo pallipes* (Fabricius) (Goeridae) offer significant variation that may be taxonomically relevant. In this species the three stout setae are straight for the basal two-thirds but then each acquires two pronounced, consecutive inflexions that introduce a kink into the seta (Fig. 112).

The hindwing costal setae vary considerably in their development, presumably in relation to the degree that they are involved with wing coupling. In Uenoidae the setae are clearly developed as coupling hooks such that in *Neophylax* spp. and *Oligophlebodes* sp. the setae are J-shaped structures arising dorsally from costa (Figs. 115–117). The setae form an evenly spaced and staggered double row and arise from well-developed sockets (Fig. 115). Based on SEM images, the sockets appear to allow for proximo-distal movement of the setae.

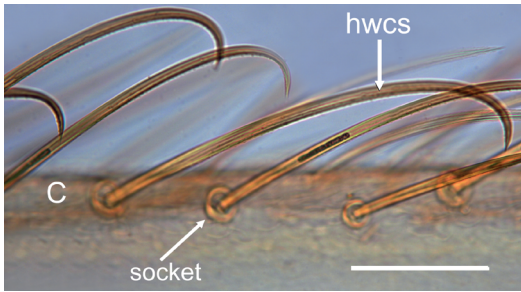


Fig. 116. LM of right hindwing coupling setae of *Neophylax ussuriensis* (Martynov) (Uenoidae), dorsal view. Scale bar = 100 μ m.



Fig. 117. SEM of the right hindwing coupling setae of *Neophylax ussuriensis* (Martynov) (Uenoidae), dorsal view. Scale bar = 10 μ m.

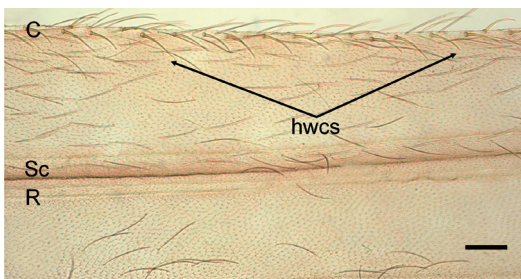


Fig. 118. LM of the right hindwing coupling setae of *Allomyia gnathos* (Ross) (Apataniidae), dorsal view. Scale bar = 100 μ m.

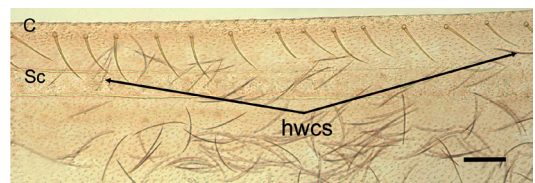


Fig. 119. LM of the right hindwing coupling setae of *Goera fuscula* Banks (Goeridae), dorsal view. Scale bar = 100 μ m.

Each socket possesses a U-shaped recess and coupling setae can be reclined into this groove along a proximo-distal axis. Functionally this may allow the setae to move fluidly with the wing as it undergoes extension during the beat cycle. Also, each seta bears distinct denticulations on the inner curvature of the hook (Fig. 117). Presumably these denticulations interdigitate with the grooves on the partner setae of the forewing. This basic morphology is present in *Allomyia gnathos* (Apataniidae; Fig. 118), *Goera fuscula* Banks (Goeridae; Fig. 119) and to a lesser extent in *Silo pallipes* (Goeridae), but these taxa differ from each other primarily in the length of the coupling setae and the fact that they are straight and do not assume the J shape found in *Neophylax* sp.

The hindwing costal setae in Limnephilidae s.s. vary more widely in their development, and by inference perhaps to the degree that they participate in wing coupling. In *Lenarchus rillus* (Milne) there is very little morphological variation in the costal setae, such that if any are

involved with coupling they are morphologically indistinguishable from the remainder of the costal setae that form a circumferential brush around costa. A slightly more differentiated series of setae is apparent in *Limnephilus fuscovittatus* Matsumura in that an evenly spaced row of fluted setae is consistently obliquely displaced from costa at $\sim 45^\circ$; in other respects they are morphologically similar to the remaining costal setae. A similar morphology obtains in *Glyphopsyche missouri* Ross, but the costal setae are clearly differentiated into two morphological groups (Fig. 120); the circumferential brush of recumbent fluted setae is diminished, but a regularly spaced row of apicoventrally oblique, fluted setae is more apparent. An intermediate condition occurs in *H. argus* in which there is both a differentiated series of evenly spaced and fluted setae projecting from costa, and a well-populated circumferential brush of recumbent setae surrounding costa (Fig. 121).

The coupling mechanism or mechanisms employed by “limnephiloid” taxa are difficult to characterize. In all taxa there is at least some interaction between the jugal lobe and prehumeral setae which probably enforces a union

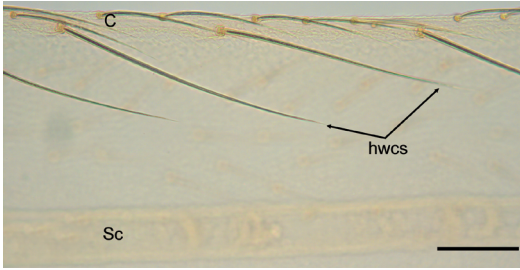


Fig. 120. LM of the right hindwing coupling setae of *Glyphopsyche missouri* Ross (Limnephilidae), dorsal view. Scale bar = 100 μ m.

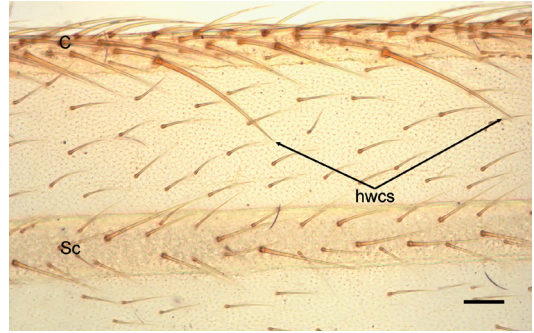


Fig. 121. LM of the right hindwing coupling setae of *Hydatophylax argus* (Harris) (Limnephilidae), dorsal view. Scale bar = 100 μ m.



Fig. 122. LM of coupled right fore- and hindwings of *Oligophlebodes* sp. (Uenoidea), dorsal view. Boxed area indicates setae in coupling position. Scale bar = 1 mm.

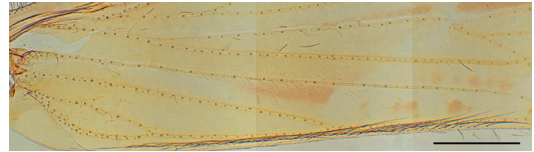


Fig. 123. LM of the left forewing of *Neophylax ussuriensis* (Martynov) (Uenoidea), showing forewing coupling setae on ambient costa, ventral view. Scale bar = 1 mm.



Fig. 124. LM close up of the left forewing of *Neophylax ussuriensis* (Martynov) (Uenoidea), showing coupling setae on ambient costa, ventral view. Scale bar = 1 mm

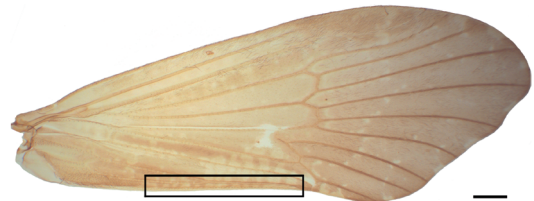


Fig. 125. LM of the left forewing of *Neophylax ussuriensis* (Martynov) (Uenoidea), ventral view. Boxed area emphasizes location of coupling setae. Scale bar = 1 mm.

of the wings on the down stroke. What may be quite variable is the level of interaction that occurs on the upstroke, which possibly ranges from nearly complete (e.g., Uenoidea) through yet-unknown degrees to little or no interaction. In Uenoidea the mechanism appears fairly straightforward in that the hooked coupling setae arranged in a row along the hindwing costa “grapple” (Fig. 122) around a circumferentially distributed bed of elongate and recumbent fluted setae that originate on the forewing ambient costa (Figs. 123–125). In Apataniidae and possibly some Goeridae (e.g., *S. pallipes*) a similar mechanism is suggested, differing primarily in the relative and variable position of the interacting groups of setae. In *A. gnathos*, *S. pallipes*

and *G. fuscula* it is the forewing setae that are elongated and linear, being positioned roughly in the plane of the wing membrane but oblique to the longitudinal wing axis at $\sim 45^\circ$ (Figs. 126–129). In these taxa the hindwing interaction is provided by a morphologically distinct class of costal setae that in some aspects of their micromorphology resemble those of Uenoidea. They differ, however, in lacking the hook-tip that results in a J-shaped profile, being instead straight to gently curved, as in *Pedomoecus sierra* (Ross) (Fig. 130), *A. gnathos* (Fig. 118) and *G. fuscula* (119). The coupling apparatus of *Apatania* sp. is markedly different in that

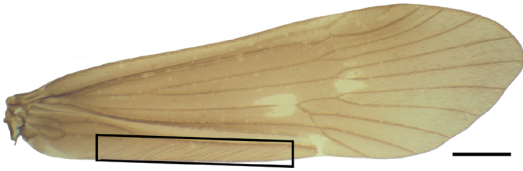


Fig. 126. LM of the left forewing of *Allomyia gnathos* (Ross) (Apataniidae), ventral view. Boxed area emphasizes location of coupling setae. Scale bar = 1 mm.

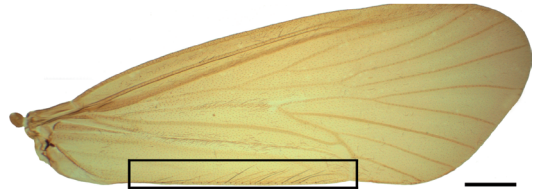


Fig. 127. LM of the left forewing of *Goera japonica* Banks (Goeridae), ventral view. Boxed area emphasizes location of the forewing coupling setae. Scale bar = 1 mm.

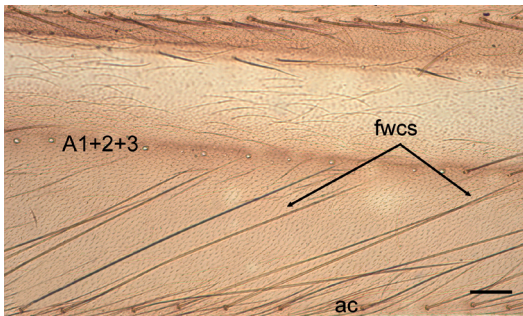


Fig. 128. LM of the left forewing coupling setae of *Allomyia gnathos* (Ross) (Apataniidae), ventral view. Scale bar = 100 μ m.

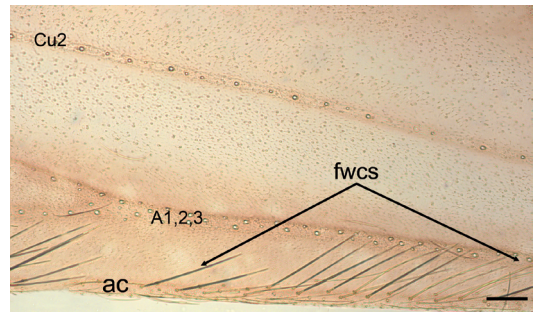


Fig. 129. LM of the left forewing of *Silo pallipes* (Fabricius) (Goeridae), showing forewing coupling setae, ventral view. Scale bar = 10 μ m.

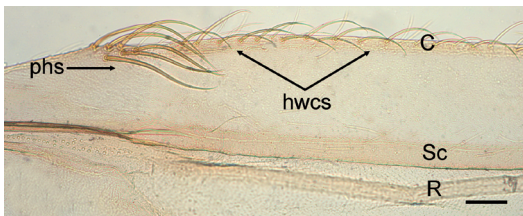


Fig. 130. LM of the right forewing prehumeral and hindwing coupling setae of *Pedomoecus sierra* Ross (Apataniidae). Scale bar = 100 μ m.

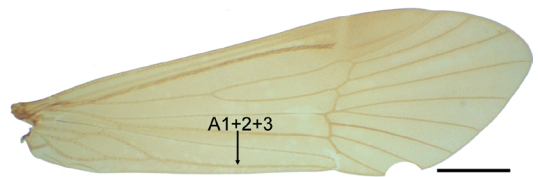


Fig. 131. LM of the left forewing of *Apatania* sp., ventral view. Scale bar = 1 mm.

the forewing coupling setae are comparatively shorter (Figs. 131 and 132), and the hindwing costal coupling setae are considerably more elongate and highly recumbent distally along the longitudinal wing axis (Figs. 133 and 134). On the forewing the coupling setae arise in a well-delimited multiserial row and originate from both ambient costa and the anal cell membrane immediately anterior to ambient costa (Fig. 132). The setae are stout and fusiform in shape and project obliquely apicoventrad at $\sim 45^\circ$ from the wing membrane.

In both Apataniidae and Goeridae the forewing-hindwing setal interaction mechanism

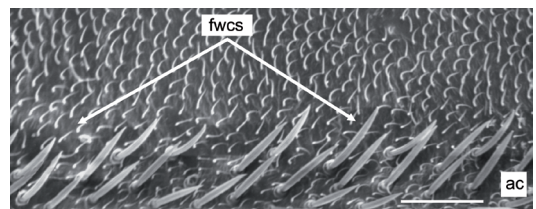


Fig. 132. SEM of the left forewing coupling setae of *Apatania cymophila* McLachlan (Apataniidae), ventral view. Scale bar = 50 μ m.

appears to be entanglement of the two setal beds. A common theme is that the two opposing beds of setae are more or less oblique to each other, generally projecting at $\sim 45^\circ$ to the longitudinal

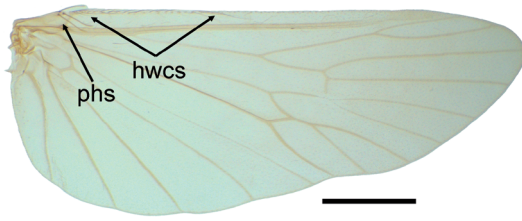


Fig. 133. LM of the right hindwing of *Apatania* sp., dorsal view. Scale bar = 1 mm.

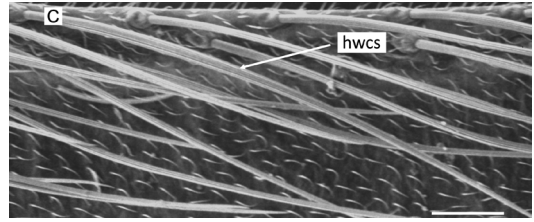


Fig. 134. SEM of the right hindwing coupling setae of *Apatania crymophila* McLachlan (Apataniidae), dorsal view. Scale bar = 50 μ m.

axis, which may serve to enhance the mechanical entanglement.

The possibility of wing coupling in Limnephilidae *s.s.* is more difficult to characterize. Like the other Limnephiloidea families, the wings are almost certainly united during the down stroke by the jugal lobe-prehumeral setae interaction, but the variable development of both the hindwing costal setae and the forewing anal cell makes for a less clear picture. Evidence that there is at least some interaction on the upstroke or the down stroke-upstroke is suggested by the wing contours and the cross-sectional profile in the forewing anal cell and hindwing costal-subcostal cell. In all Limnephilidae *s.s.* taxa examined, the forewing anal cell is basally more or less parallel-sided, bounded by linear A1+2+3 and ambient costa veins (Figs. 101–103); similarly, the hindwing costal-subcostal cell is approximately parallel sided, at least basally, with a linear costa. In *P. sonso*, the wing membrane in cross section in these cells is menisciform; the forewing anal cell membrane is ventrally convex, dorsally concave, and the membrane of the hindwing cell is flat to slightly dorsally concave. When superimposed in the open position the wings overlap such that the two cells are approximate. In such a position, hindwing costa is superimposed on the forewing anal cell, and the forewing ambient costa is approximate to the hindwing subcosta and Radius. In this position the opposing fields of socketed setae are brought into close approximation, which then become enmeshed (Fig. 104).

Such approximation may be sufficient to result in some measure of coupling, but additional coupling support may be derived from the hindwing costal setae interacting with socketed setae populating the forewing anal cell. The

degree of development of the anal cell setae and the hindwing costal setae vary widely among taxa, from sparse to dense beds of weakly developed setae, to more stoutly developed setae; in all cases examined the setae are oriented at $\sim 45^\circ$ to the longitudinal wing axis.

Discussion

With the exception of work by Vineyard and Wiggins (1988) (Uenoidae), Huxley and Barnard (1988) and Johanson (1998), there has been no attempt to extract either taxonomically or phylogenetically useful information from the morphology of the putative WCA of integripalpiian taxa. Results presented here suggest that these structures present a bounty of data for not only comparative morphologists, but also for functional and experimental morphologists that wish to study the evolution of complex interacting fields of morphology. Even without a taxonomically in-depth survey, numerous structures have been identified that can provide both taxonomically and phylogenetically valuable data.

Especially variable in Breviventoria is the development of the jugal lobe, varying from a well-developed structure in Phryganeidae and allied families to a relatively diminished structure in Limnephilidae and allied families. The functional role has probably also been modified, but the presumed outcome remains that it is involved with ensuring the union of the wings during the down stroke. Within the “limnephiloid” families Apataniidae and Goeridae, there is also an interesting mix of morphologies that at present eliminates their use as synapomorphies; the development of the forewing and hindwing coupling setae at some level probably represents

homology, but their divergent development in different clades suggests a highly homoplastic system. The prehumeral setae show sufficiently varied morphology that they could be useful in establishing sub-family grade clades; this appears especially so for the distinctive setae in *Apatania* sp. and *Apataniana* sp. The J-shaped coupling hook morphology in *Neophylax* sp. and *Oligophlebodes* sp. might, if more taxa are sampled from additional genera, provide a family-level synapomorphy.

Four major evolutionary themes are developed in the morphology of Brevitentoria–diminution of the forewing jugal lobe, diminution of the prehumeral setae, enhancement of ambient costa and development of a bed of microtrichia on the forewing anal angle.

The lobe of the anal angle of Philorheithridae may or may not be a homologue of that in other taxa, such as Calamoceratidae, Leptoceridae and Odontoceridae, but its remarkable development within philorheithrid taxa makes it a strong candidate for a synapomorphy. The morphological theme of development of the forewing anal angle microtrichia is also probably related to the general augmentation of ambient costa. This vein, which in most brevitentorian and annulipalpi families is only weakly developed, becomes much more pronounced, deviates from the plane of the wing ventrally, and becomes densely populated with microtrichia. Overall it presents a stout, lip-like structure that can apparently provide a well-developed grip on partner structures of the hindwing. Development of this type, which is common in both sericostomatoid and “leptoceroid” families, is particularly evident in Molannidae, Leptoceridae, Helicopsychidae, Chathamidae and Calocidae, in which families the ambient costa vein itself, and not setal structures developed from it, serves as the forewing coupling component. The morphological outcome is to present a trough-like structure into which hindwing coupling setae are inserted. The development of this complex of structures (ambient costal vein, pseudovein cuticular neoformations, A1+2+3) should be documented in a more extensive group of taxa, and doing so may improve the phylogenetic resolution of this complex for several of the sericostomatoid families in particular.

Also of interest is the relationship between morphology and function when there is the possibility that multiple functional roles are fulfilled by a structure or complex of structures. The evolution of wing coupling may have been potentiated by the fact that several of the constituents of a coupling system may have had prior functional roles. In particular, the lobe adjacent to the forewing anal angle in Philorheithridae is employed in a functional role similar to that assumed by the microtrichia fields in the anal cell of *Smicridea* sp. (Hydropsychidae: Smicrideinae; Stocks 2009). In *Kosrheithrus tillyardi* and *Austrheithrus dubitans* the lobe is employed as a friction-based releasable fastener (*sensu* Gorb *et al.* 2002) that maintains the wings in the tectiform position; the topology and vestiture of the lobes is such that they intermesh and form a robust connection. Similar and possibly homologous lobes occur in Leptoceridae and Odontoceridae in particular, but are less well developed. However, in Leptoceridae the patch of microtrichia is drawn out extensively along ambient costa and forms the forewing component of the forewing-hindwing coupling apparatus. Thus it is possible that a structure involved with one function (at rest forewing-forewing coupling) came to be employed as part of a forewing-hindwing coupling system.

In general, taxa that do not couple their wings may still display significant forewing-hindwing interaction, and insight into the origins of the coupling mechanisms can be gained by examining the relevant structures across trichopteran taxa. From this perspective the repeated evolution of diptery as a form-functional complex will be seen as the result of sequential exaptation (*sensu* Gould & Vrba 1982), with functional diptery as an outcome that has been repeatedly realized by different combinations of anatomic structures. Considering that wings of insects in general are equipped with a diverse tool-box of morphological attributes (e.g., socketed setae, both enervated and unenervated, wing membrane cuticle with differential sclerotization, taxonomically variable venation, sculpting of micro-morphological properties of the cuticle, and variation in physical properties like rigidity), it is less surprising that caddisfly lineages of varying phylogenetic distance should have converged on a similar functional capacity.

Wing coupling apparatuses that yield functional diptery are only one class of biomechanical interactions that are known in insect functional biology (reviewed by Gorb 2001). Biomechanical interactions between the wing-body and wing-wing are well known in numerous insect groups, and are examples of friction-based releasable attachment devices (Gorb *et al.* 2002). Collectively, these micotrichia- and/or setae-based biomechanical locks are known as “probabilistic” since they do not require a precise correspondence between parts in order to function (Gorb *et al.* 2002). The biomechanical properties of these systems are understood in several taxa and suggest a particular function in an ecological scenario. For example, *Merope tuber* Newman (Meropeidae: Mecoptera) has cuticular ridges on the forewing jugal lobe and metascutellum which, when in contact, interdigitate and serve to lock the wings dorsally over the body. This morphology is presumed to correlate with their ecology as substrate dwellers that move in tight spaces, in which circumstances the wings are prone to disruption and entanglement in substrate debris (Hlavac 1974). Heteroptera may have either or both types of locking devices in addition to forewing-hindwing coupling structures, and in some aquatic Heteroptera the wing-wing and wing-body locks form a seal sufficiently tight to retain an air pocket while submerged (Gorb & Perez Goodwyn 2003). A diversity of locking mechanisms also occurs in Lepidoptera, the most well-known being the at-rest wing- and- body-locking mechanism that is comprised of a dense patch of strong microtrichia on the ventral surface of the forewing anal cell, and that is partner to a patch of microtrichia on the metascutum (Kuitjen 1974). Presence of this mechanism was shown to correlate with the resting position assumed by the insect; moths that kept their wings “closely pressed against the thorax” possessed the mechanism, and was absent in moths that held their wings less closely to the thorax (Kuitjen 1974).

Two mechanisms in particular can be discussed that appear to be functional analogues of the forewing-forewing coupling apparatus of many Trichoptera. Certain Aphelinidae and Encyrtidae (Hymenoptera: Chalcidoidea) possess a forewing-forewing locking mechanism

based on a seta-retinaculum interaction (Hennessey 1981). The phylogenetic distribution of wing locking was found to correlate with the propensity to parasitize homopterous insects, leading the author to hypothesize that there was adaptive value to wings that lock securely in place, arguing that they would be less likely to become entangled in sticky honeydew secreted by the host. Several Belostomatidae (Heteroptera) taxa (e.g., *Lethocerus* spp., *Abedus* spp.) lock the forewings (hemelytra) together with a “brush-to-brush frictional surface” system (Gorb & Perez Goodwyn 2003), in which two opposing patches of distinctively shaped setae become entangled. In both the Chalcidoidea and Belostomatidae wing-locking systems there is no inherent bias in which wing is superior while locked in place.

That a form-functional complex in at least some Trichoptera is involved with retaining the wings at rest is suggested by several lines of morphological evidence that collectively illustrate that the wings, which generally appear to be flat surfaces, in fact assume complex topologies. An alternative modality is also suggested by evidence from *in vitro* manipulation wherein the wings are resistant to separation under gentle pulling, but will eventually separate abruptly if pulled sufficiently.

Comparative analyses reveal that the bed of densely and variously developed microtrichia near the forewing anal angle is widely distributed in Trichoptera, but appears to be particularly well developed in Brevitentoria (Integripalpia); the bed and morphology of the anal angle is so distinctive in Philorheithridae that it is offered as a family-level synapomorphy (Weaver *et al.* 2008). The biomechanical principle appears to rely on the fact that the lobes are dorso-ventrally menisciform in shape, which allows the dorsal surface of one lobe to rest on the ventral surface of the opposite lobe. Thus, the two opposing fields of microtrichia are then approximate and become entangled. Entanglement, and therefore stability, is probably enhanced by the fact that the microtrichia are strongly curved and pointed. There are few ecological or behavioral observations on adults that could shed light on the role of coupled forewings, but philorheithrids are known to rest on twigs with their wings held tightly to the body, similar to that attained by molannids when at

rest. Alternatively, or additionally, wings closely attached to the body might enable the animals to move through tight underbrush more efficiently or with decreased risk of damage to the wings, a role similar to that in Meropeidae.

Other morphological considerations may also bear on the issue. Interacting fields of microtrichia and setae in the ventral anal cell and on hindwing costa form the basis of the putative forewing-hindwing coupling mechanism in Limnephilidae; when in the *coupled* position, the menisciform (in transverse section) anal cell of the forewing is approximate to the hindwing costal-subcostal space and parallels the costal and subcostal vein. However, when the wings are in the *tectiform* position, they assume a confirmation similar to that of Phryganaeidae, in which the two menisciform surfaces, each replete with microtrichia, become approximate and parallel to the longitudinal body axis. In such a position the menisciform surfaces are superimposed, and presumably securely locked in place over the back. Both Phryganaeidae and Limnephilidae also possess a forewing jugal lobe and hindwing prehumeral bristles and presumably fly with these structures engaged, resulting in coupled wings on the down stroke. Thus, the constituent elements of a forewing-hindwing coupling system are already present in a form-functional complex and available to the phenomenon of exaptation (Gould & Vrba 1982).

Acknowledgements

I gratefully acknowledge the assistance of P. H. Adler, R. W. Blob, J. C. Morse and C. R. Parker. A. P. Wheeler provided access to the electron microscope. Acknowledgements are also extended to reviewers who critiqued the manuscript and offered suggestions for its improvement. This is Technical Contribution No. 5718 of the Clemson University Experiment Station.

References

- Gorb, S. N. 2001: *Attachment devices of insect cuticle*. — Kluwer Academic Publishers Dordrecht, Boston, London.
- Gorb, S. N., Beutel, R. G., Gorb, E. V., Jiao, Y., Kastner, V., Niederegger, S., Popov, V. L., Scherge, M., Schwarz, U. & Voetsch, W. 2002: Structural design and biomechanics of friction-based releasable attachment devices in insects. — *Integrative and Comparative Biology* 42: 1127–1139.
- Gorb, S. N. & Perez Goodwyn, P. J. 2003: Wing-locking mechanisms in aquatic heteroptera. — *Journal of Morphology* 257: 127–146.
- Gould, S. J. & Vrba, E. S. 1982: Exaptation — a missing term in the science of form. — *Paleobiology* 8: 4–15.
- Hennessey, R. D. 1981: At-rest seta wing coupling and restraining mechanisms in the Encyrtidae and Aphelinidae (Hymenoptera: Chalcidoidea). — *Annals of the Entomological Society of America* 74: 172–176.
- Hlavac, T. F. 1974: *Merope tuber* (Mecoptera): a wing-body interlocking mechanism. — *Psyche* 81: 303–306.
- Holzenthal, R. W., Blahnik, R. J., Kjer, K. M. & Prather, A. L. 2007a: An update on the phylogeny of caddisflies (Trichoptera). — In: Bueno-Soria, J. R., Barba-Álvarez, J. R. & Armitage, B. (eds.), *Proceedings of the 12th International Symposium on Trichoptera*: 143–153. The Caddis Press Publishers.
- Holzenthal, R. W., Blahnik, R. J., Prather, A. L. & Kjer, K. M. 2007b: Order Trichoptera Kirby, 1813 (Insecta), Caddisflies. — *Zootaxa* 1668: 639–698.
- Huxley, J. & Barnard, P. C. 1988: Wing-scales of *Pseudoleptocerus chirindensis* Kimmins (Trichoptera: Leptoceridae). — *Zoological Journal of the Linnean Society* 92: 285–312.
- Ivanov, V. D. 1991: Evolution of flight in caddisflies. — In: Tomaszewski, C. (ed.), *Proceedings of the Sixth International Symposium on Trichoptera*: 351–357. Adam Mickiewicz University Press, Poznań.
- Johanson, K. A. 1998: Phylogenetic and biogeographical analysis of the family Helicopsychidae (Insecta: Trichoptera). — *Entomologica Scandinavica Supplement* 53: 1–172.
- Kjer, K. M., Blahnik, R. J. & Holzenthal, R. W. 2002: Phylogeny of the caddisflies (Insecta, Trichoptera). — *Zoologica Scripta* 31: 83–91.
- Kuitjen, P. J. 1974: On the occurrence of a hitherto unknown wing-thorax coupling mechanism in Lepidoptera. — *Netherlands Journal of Zoology* 24: 317–322.
- Morse, J. C. 2003: Trichoptera (caddisflies). — In: Resh, V. H. & Cardé, R. T. (eds.), *Encyclopedia of insects*: 1145–1151. Academic Press, San Diego.
- Morse, J. C. 2009: *Trichoptera world checklist*. — Available at <http://entweb.clemson.edu/database/trichopt/index.htm>.
- Mosely, M. E. 1936: Tasmanian Trichoptera or caddis-flies. — *Proceedings of the Zoological Society of London* 2: 395–424.
- Scheffer, P. W. 1996: Phylogenetic relationships among subfamily groups in the Hydropsychidae (Trichoptera) with diagnoses of the Smicrideinae, new status, and the Hydropsychinae. — *Journal of the North American Benthological Society* 15: 615–633.
- Schmid, F. 1998: *Genera of the Trichoptera of Canada and adjoining or adjacent United States*. — NRC Research Press, Ottawa.
- Stocks, I. C. 2009: Comparative and functional morphology of wing coupling and related structures in caddisflies (Trichoptera): Annulipalpia. — *Journal of Morphology* 271: 152–168.

- Tillyard, R. J. 1918: The Panorpid complex. Part I. The wing coupling apparatus, with special reference to the Lepidoptera. — *Proceedings of the Linnaean Society of New South Wales* 43: 286–319.
- Vineyard, R. N. & Wiggins, G. B. 1988: Further revision of the caddisfly family Uenoidae (Trichoptera): evidence for inclusion of Neophylacinae and Thremmatinae. — *Systematic Entomology* 13: 361–371.
- Vshivkova, T., Morse, J. C. & Ruiter, D. 2006: Phylogeny of Limnephilidae and composition of the genus *Limnephilus* (Limnephilidae: Limnephilinae, Limenphilini). — In: Bueno-Soria, J. R., Barba-Álvarez, J. R. & Armitage, B. (eds.), *Proceedings of the 12th International Symposium on Trichoptera*: 309–319. The Caddis Press Publishers.
- Weaver, J. S. III, Gibon, F.-M. & Chvojka, P. 2008: A new genus of *Philorheithridae* (Trichoptera) from Madagascar. — *Zootaxa* 1825: 18–28.
- Wiggins, G. B. 1968: Contributions to the systematics of the caddisfly family Molannidae in Asia (Trichoptera). — *Royal Ontario Museum, Life Sciences Contributions* 72: 1–26.